Are perineuronal nets in the medial prefrontal cortex critical for the prepulse inhibition of the acoustic startle reflex in mice?

Master thesis in Molecular Bioscience

Main field of study in physiology and neurobiology

Christopher Ortega Stensrud

60 credits

Program for Physiology and Neurobiology
Department of Biosciences
The Faculty of Mathematic and Natural Sciences

UNIVERSITY OF OSLO

2018

Are perineuronal nets in the medial prefrontal cortex critical for the prepulse inhibition of the acoustic startle reflex in mice?

Christopher Ortega Stensrud

Program for Physiology and Neurobiology

Department of Biosciences UNIVERSITY OF OSLO

September 2018

2018

Are perineuronal nets in the medial prefrontal cortex critical for the prepulse inhibition of the acoustic startle reflex in mice?

Christopher Ortega Stensrud

http://www.duo.uio.no/

Print: Reprosentralen, University of Oslo

Acknowledgments

The work presented in this thesis was conducted at the Program for Physiology and Neurobiology at the Department of Biosciences, University of Oslo between October 2016 and September 2018, under the supervision of associate professor Dr. Marianne Fyhn, Dr. Martha Hvoslef-Eide and PhD fellow Elise Holter Thompson.

First and foremost, I would like to thank my supervisors Marianne Fyhn, Martha and Elise. Your contributions to my thesis have been indispensable. To Marianne, thank you for accepting me as part of your neuroscience research group, granting me freedom and resources to design my own experiments and for your valuable knowledge and guidance. To Martha, thank you for providing me the tools to get started with my project and setting up the base of operations, the skills you have taught me, guidance in writing my thesis, pushing me towards becoming an independent student and for the time you have invested in me. To Elise, thank you for supervising me under the absence of Martha and following up on my thesis to the very end, your guidance, for always being helpful and making me feel as a part of the team.

Secondly, I would like to thank all the people of CINPLA and the Hafting/Fyhn group. Especially those who at any point found themselves involved in any aspect of my master's project, including Jennifer Hazen, Kristian Lensjø, Sverre Grødem, Marte Julie Sætra and Ulrike Schlegel.

I would also like to extend my gratitude to my co-students and friends, including Ulrike, Hallvard, Evan, Laura, Teeh, Arne and Nuria for your valuable friendship and many great moments.

Lastly, I want to thank my fiancée and family for their extraordinary support.

Oslo, September 2018

Christopher Ortega Stensrud

Abstract

Schizophrenia (SCZ) is a chronic and severe brain disorder with a complex pathophysiology. Some clinical symptoms of SCZ patients have been associated with behavioural, physiological and anatomical deviations in the medial prefrontal cortex (mPFC) including, but not limited to, lower expression of perineuronal nets (PNNs) and impaired sensorimotor gating. Animal models of the disorder mirror these deficits, whilst also demonstrating abnormal inhibitory neuron activity.

Sensorimotor gating is the process of regulating transmission of sensory input from environmental stimuli to a motor system. Sensorimotor gating can be assessed experimentally by studying the startle response and measuring the inhibitory effects of a weak sensory stimulus preceding a strong sensory stimulus, a task called Prepulse inhibition (PPI). This inhibitory effect is disrupted in SCZ; the startle response is similar regardless of the existence of a weak stimulus preceding the strong.

The PNNs are specialized extracellular matrix structures surrounding a subset of neurons, mostly parvalbumin positive inhibitory neurons (PV+ cells), in the central nervous system. The removal of PNNs cause a disruption of PV+ cell activity, leading to a dysfunctional inhibitory circuitry. Recent studies have found reductions in mPFC PNN levels as a result of ketamine exposure in a rat model of SCZ (Matuszko et al., 2017), and that PNNs in mPFC mature in adolescence, coinciding with the typical age of onset of SZ (Baker et al., 2017). Whilst decreased levels of PNNs and PPI impairments are both associated with SCZ, it is not known if reduced expression of PNNs may explain the impairment of PPI in SCZ. The fast spiking phenotype of GABAergic PV+ cells is aided by the presence of PNNs and removal of PNNs leads to a decrease in inhibitory activity (Favuzzi et al., 2017; Lensjø et al., 2017b). Moreover, decreased levels of GABAergic signaling is a well-known pathology in SCZ (Perry et al. 1979), a malfunction correlated with the inability to coordinate information processing among brain areas (Haig et al., 2000).

In light of this, the current study investigated whether reduced expression of PNNs in mPFC could contribute to impairments in PPI as a measure of sensorimotor gating. To achieve this, we utilized a transgenic mouse line which allowed targeted deletion of the gene for aggrecan, a key protein in the PNN structure, causing selective and stable removal of PNNs in the mPFC. Moreover, as PPI involves a widespread brain network, we tested PPI in mice in PV+

cell-specific, brain-wide aggrecan knockout that never develops PNNs around PV+ cells (Acan/PV KO). To compare effects of the interventions on sensory responses to sound stimuli, animals were exposed to sounds of increasing sound pressure levels in a sound-pressure sensitivity test.

In mice without PNNs around the PV+ cells, the Acan/PV KO group~~,~~ showed stronger startle responses in the sound-pressure sensitivity test compared to all other groups. These findings indicate role for PNN in development of sensory processing ensuring normal reaction pattern to the sensory environment. Absolute PPI startle responses were lowered as a consequence of aggrecan knockout in the mPFC. In contrast, no effect was observed on PPI neither in the brain-wide knockout or the local removal of aggrecan in mPFC.

These preliminary results may indicate that distorted PNN expression of SCZ patients may be associated with sensory processing deficits in these patients, but the subtle intervention caused by PNN removal in the adult mPFC was overruled by stronger processing mechanisms in other parts of the brain network responsible for PPI. This shows that the lack of PNN development around PV+ cells has affected the sound-pressure sensitivity test, an effect not observed when PNN removal was restricted to mPFC.

In conclusion, these results indicate that the development of PNNs around PV-cells is crucial for the development of a normal sensory processing system; however, PNN deficiency does not disrupt sensorimotor gating.

Table of contents

1. Introduction

1.1. Schizophrenia

Schizophrenia (SCZ) is a chronic, severe and disabling neuropsychiatric disorder which has a profound effect on afflicted individuals and represent large societal costs. The disease is thought to affect 0.7% of the world's population (MacDonald et al., 2009). The disorder is one of the leading causes of disability, with rates of unemployment at 80-90% in Europe (Marwaha et al., 2004). In England alone, it is estimated that £12 billion are spent on SCZ every year, with roughly one third accounted for by health and social care ("The Schizophrenia Commission - Rethink Mental Illness, the mental health charity," 2012). The average life expectancy of people with SCZ has been reported to be about 20 years lower than the general population (Tiihonen et al., 2009). While SCZ has strong heritability (Litchenstein et al., 2009), both genetic and environmental factors contribute to the aetiology of SCZ. The underlying mechanisms of SCZ are far from understood and efficient, targeted treatments are limited. For example, SCZ patients on second-generation antipsychotic drugs had only a marginal extension of life expectancy by 2.5 years (Tiihonen et al., 2009).

The disorder has a heterogeneous presentation of trademark positive, negative and cognitive symptoms. The positive symptoms include hallucinations, delusions and disorganized thinking, speech and behavior, whereas the negative symptoms include social withdrawal, affective flattening and poverty of speech (alogia). Additionally, impaired psychomotoric speed, attention, memory and executive functioning encompass the cognitive symptoms (Heinrichs & Zakzanis, 1998).

A series of physiological and functional abnormalities have been associated with certain brain areas in patients diagnosed with SCZ, including the prefrontal cortex, a brain region involved in sensorimotor gating. A central finding is the reduced brain oscillations in the gamma frequency range (30-200 Hz) found in all stages of SCZ. Gamma oscillations are, among other functions, proposed to be necessary for sharing information across brain areas (Williams & Boksa, 2010). Anatomical disturbances have also been linked to SCZ. Reduced dendritic spine densities on pyramidal neurons in input layers of the prefrontal cortex was observed in post mortem investigations of SCZ patients (Lewis et al., 2003). Moreover, lower densities of

perineuronal nets, a tight lattice of extracellular matrix enwrapping specific neurons, are among the more robust findings in SCZ patients where mPFC seems to be among the brain regions most affected (Mauney et al., 2013; Berretta et al., 2015). This is in line with impaired performance of SCZ patients in prefrontal cortex-dependent tasks, such as the continuous performance task, (MacDonald et al., 2005; Delawalla et al., 2008). Moreover, patients with SCZ exhibit impaired prepulse inhibition (PPI), an operational measure of sensorimotor gating functioning (Geyer and Braff., 1987; Swerdlow & Geyer., 1998; Braff et al., 2001; Swerdlow et al, 2017). Sensorimotor gating is a basal function of pre-attentive regulation of transmission of sensory information to a motor system, that is conserved across species making it an ideal target for translational studies (Landis and Hunt., 1939; Nusbaum & Contreras., 2004).

1.2 Prepulse inhibition of the acoustic startle response

Constant adaptation to sensory stimuli from the environment is required in order for an animal to retain appropriate focus, and to ensure correct responses to sudden changes. Prepulse inhibition (PPI) is a measure of how a startle reflex to an intense stimulus can be weakened when preceded by a weak stimulus (Swerdlow & Geyer., 1998). PPI is regulated by neural inhibition and has been shown to be impaired in patients with SCZ (Geyer and Braff., 1987).

1.2.1 The acoustic startle reflex

The acoustic startle reflex (ASR) is a rapid, unconditioned response evoked by the presentation of an unexpected intense auditory stimulus. The startle reflex is a response that is thought to protect an organism from danger and prepare for a fight-or-flight response. The ASR manifests itself as a jerk-like motor reflex with rapid contraction of facial, neck and skeletal muscles, accompanied by increased heart rate and arrest of ongoing behaviors. The ASR is fundamental for survival and appears to be evolutionary conserved as it is found from invertebrates, to fish to all mammalian species that have been studied (Landis and Hunt., 1939; Hoy et al., 1989., Burgess and Granato, 2007). The ASR is elicited by high intensity acoustic stimuli, typically over 80 dB sound pressure level (SPL) at all frequencies in the audible range with a steep rise time (Pilz et al., 1987). The onset latency of the ASR is very

fast (5-10 msec) (Caeser et al., 1989) and is therefore mediated by a short and simple neural circuit in the lower brainstem. (Yeomans and Frankland., 1995) (Figure 1.1).

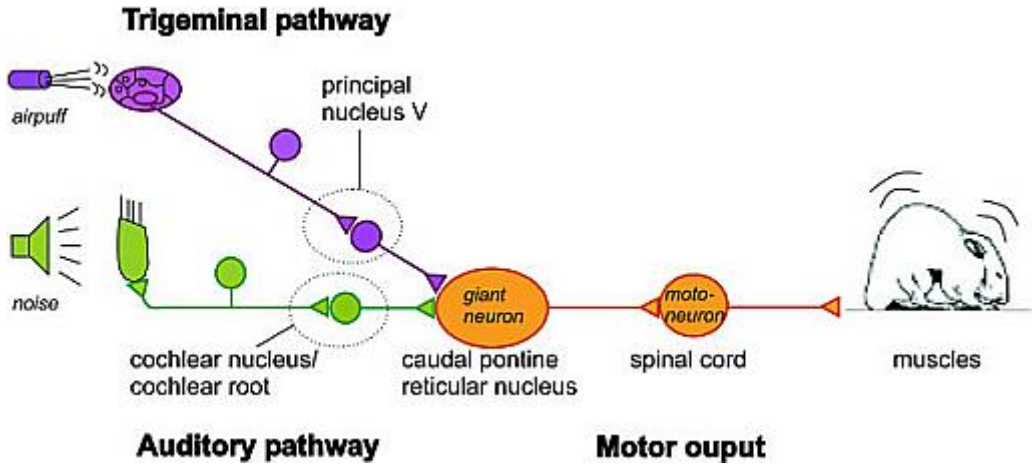

Figure 1.1: The primary ASR pathway. Acoustic information is conveyed by primary neurons in the auditory nerve to the cochlear nuclear complex, and then to the caudal pontine reticular nucleus, where they converge onto giant neurons that project onto spinal motor neurons to carry out the startle response. Figure from https://openi.nlm.nih.gov/detailedresult.php?img=PMC1479352_1471-2202-7-38-1&req=4

1.2.2 Modulation of the acoustic startle reflex and sensorimotor gating

The ASR amplitudes vary between individuals (Plappert et al., 1993) and are influenced by genetic differences (Glowa and Carl., 1994). Additionally, the response magnitude is very prone to internal and external modulation. Ongoing motor behaviors (Wecker and Ison., 1986), changes in the perceptual or emotional state (Davis et al., 1997) and drug exposure (Davis., 1980), are just a few of many factors that have been found to affect startle reflex amplitudes.

The response amplitude can be modified because of sensorimotor gating, a process in which the organism adapts to changes in the sensory environment to give the appropriate response (Swerdlow & Geyer., 1998). Sensorimotor gating is a physiological process in which sensory information is filtered as it is transmitted to motor output systems. It is a protective mechanism against information overload and cognitive fragmentation (Cryan and Reif., 2012). The startle response plays an important role in behavioral plasticity and is used as a tool to map healthy and pathological sensorimotor gating. The ASR is well suited as an experimental model to investigate information processing because of its simple response

being evoked by stimuli that are easy to control and automate (Geyer and Braff., 1987; Braff & Geyer., 1990). Moreover, it is an instructive measure of information processing and inhibitory function in sensorimotor gating (Swerdlow et al 2008; Braff., 2010). Impaired sensorimotor gating is considered a hallmark trait in SCZ (Swerdlow et al., 2017), making ASR a valuable tool to assess neuropathological dysfunctions in SCZ (Geyer and Braff., 1987). Furthermore, studies have found that second generation antipsychotic medication normalizes PPI in SCZ patients (Kumari et al., 2000; Weike et al., 2000).

1.2.3 Prepulse inhibition

Prepulse inhibition can be measured when a weak stimulus is presented prior to a strong stimulus, to inhibit or dampen the response to the strong stimulus. An example is the reduction of ASR to a loud sound (a startle pulse) when it is preceded by a lower sound (non-startle prepulse) (Figure 1.2). PPI is measured as the drop in ASR amplitude:

A high PPI indicates strong sensorimotor gating because the ASR amplitude relative to the amplitude of the startle pulse is decreased when preceded by a non-startle prepulse (Braff & Geyer., 1990; Cadenhead, Geyer, & Braff., 1993; Swerdlow & Geye.r, 1998). In people with SCZ, disturbed sensorimotor gating manifests as impaired PPI, consequently leading to similar ASR whether the startle inducing stimulus is preceded by a prestimulus or not (Geyer and Braff., 1987).

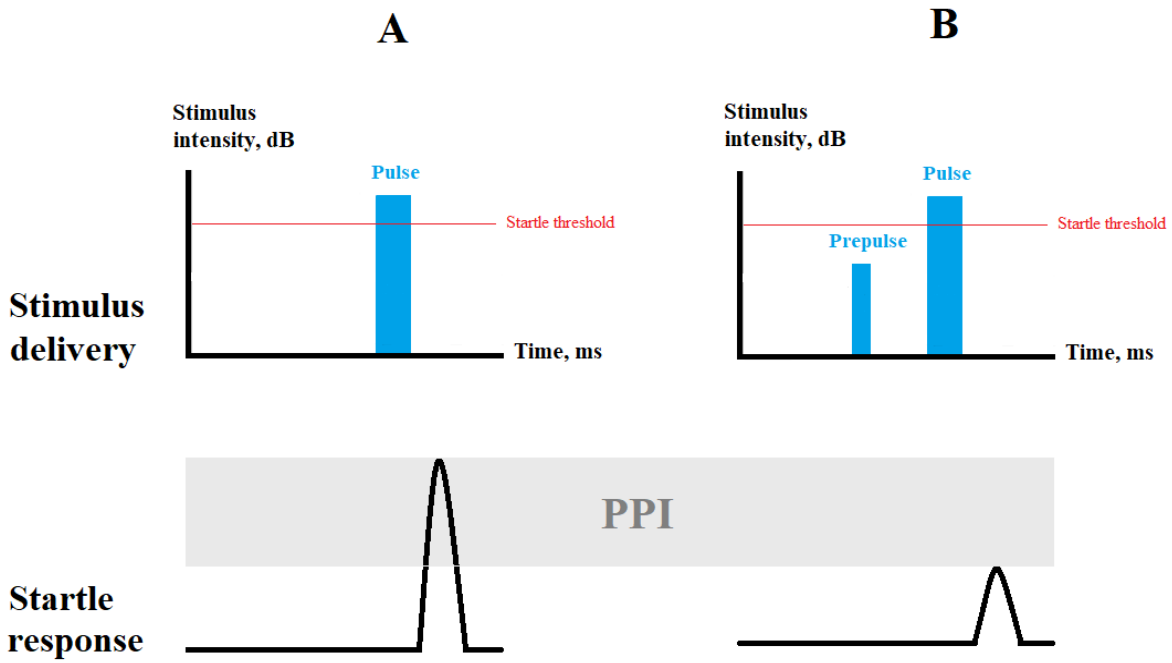

Figure 1.2: The prepulse inhibition (PPI) of the ASR. (A) When a subject is exposed to a sound pulse that is above startle threshold, the subject demonstrates a pronounced startle response. (B) When a startle-inducing pulse is preceded by a sub-startle threshold prepulse, the startle response is reduced. This difference in the ASR is known as PPI, and the magnitude of PPI is proportional to the difference in startle response between the two (gray). The stimulus event must be conducted under a brief temporal window for the stimulus-coupling paradigm to work, typically 100-200 msec and no longer than 500 msec.

As an operational measure of sensorimotor gating, PPI is highly reliable, requires no training, and is easily observed in rodents and humans with the same stimulus parameters to generate equal response patterns (Hoffman and Ison., 1980; Dawson, Schell, & Böhmelt., 1999). The ASR and PPI can therefore be reliably quantified and compared across species and is therefore a good model for translational investigations. The ASR is typically indexed in humans with electromyography by measuring the contraction of the muscle that closes the eye, an important part of the startle reflex (Ison and Pinckney., 1983). In rodents, on the other hand, the ASR is quantified and indexed by placing the animal on a load-cell platform that transduces the downward force resulting from the whole-body skeletal muscle contraction of the startle (Willot, et al., 2003).

PPI is regulated by a large inter-connected circuitry composed of cortex, thalamus, striatum and pallidum, as studies through extensive preclinical rodent work over many decades (Swerdlow et al., 2016). It is beyond the scope of this thesis to go into detail on the PPI circuitry, but disruption of PPI has been connected to malfunctions of the nucleus accumbens and the medial prefrontal cortex (mPFC) (Swerdlow et al., 2016) as indicated in SCZ. The

indirect evidence linking mPFC dysfunction to PPI in SCZ patients is supported by causal lesions of the mPFC in rats, which is sufficient to impair PPI (Bubser et al., 1994).

1.3 Perineuronal nets

The perineuronal net (PNN) is a type of extracellular matrix (ECM) that wrap around a subset of neurons in the central nervous system (Golgi, 1898).The net is made of sugar chains and proteins that form a tight mesh covering the surface of the soma and proximal dendrites (Hendry et al., 1988; Watanabe et al., 1989; Balmer et al., 2009) with openings for synaptic connections onto the neuron. It mainly enwraps fast spiking GABAergic parvalbumin-expressing (PV+) inhibitory interneurons in the cortex (Celio., 1986; Dityatev et al., 2007; Wang et al., 2012), with some exceptions such as area CA2 of the hippocampus where they are found around pyramidal cells (Carsten et al, 2016; Lensjø, et al., 2017a).

The PNN structure consists of hyaluronan, chondroitin sulfate proteoglycans (CSPGs), tenascin-R and link proteins (Carulli et al., 2006; Deepa et al., 2006, Kwok et al., 2011) (Fig 1.3). There are four different types of CSPGs found in PNNs, aggrecan, neurocan, brevican and versican, the main one being aggrecan. Aggrecan is mainly expressed by the PV+ inhibitory interneurons (PV+ cells), and PNN formation around PV+ cells is dependent on aggrecan expression (Carulli et al., 2006; Giamanco & Matthews., 2012).

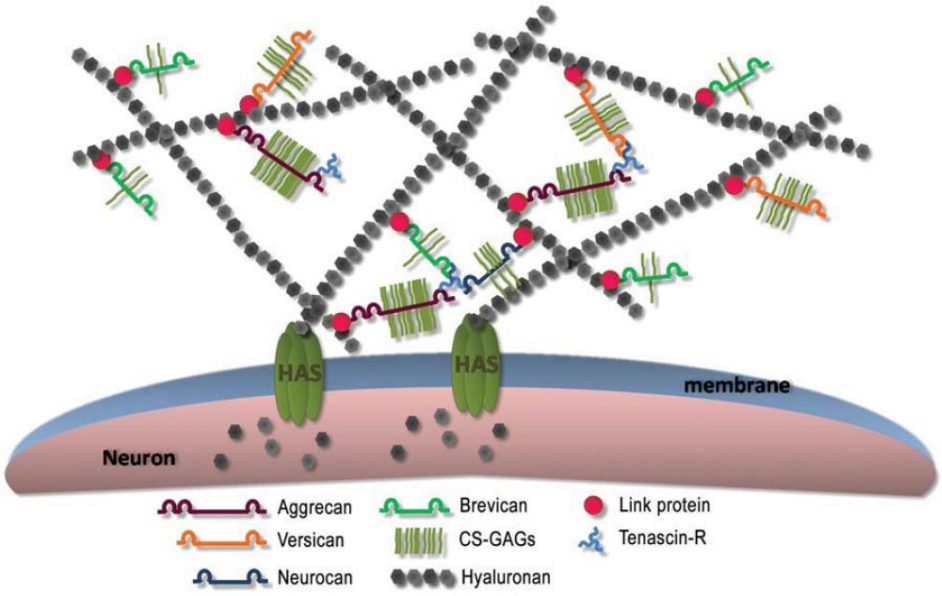

Figure 1.3: The structure of perineuronal nets (PNNs). The PNN backbone is composed of long chains of hyaluronan. Link proteins then connect the negatively charged CSPGs to the backbone and the trimeric Tenascin-R secure CSPGs to each other. Figure from Kwo et al. (2011).

Condensation of PNNs and maturation of inhibitory neurons coincides with closure time restricted periods of heightened plasticity in the juvenile brain called "critical periods" (Hensch., 2005; Pizzorusso et al., 2006; Wang, et al., 2012; Lensjø et al., 2017b). Sensory cortices show pronounced critical period plasticity followed by low adult plasticity. Removal of PNNs from e.g. primary visual cortex in the adult brain reopens critical period plasticity (Pizzorusso et al., 2002; Lensjø et al. 2017b).

Although the proteins of PNNs are long lived, the PNNs are likely finely regulated and continuously modified to meet the need for brain plasticity. PNN re-modeling is under control of the activity of endogenous enzymes called metalloproteinases that may partially degrade the nets during periods of learning when there is need for a more plastic environment (Meighan et al., 2006). Removal of PNNs in different brain areas has been shown to affect learning and memory processing (Gogolla et al., 2009; Hylin et al., 2013; Slaker et al., 2015, Thompson et al., 2018).

The effect of PNNs on plasticity is likely through facilitating optimal conditions for the fast-spiking activity of PV+ cells, fine tuning the excitatory-inhibitory balance of neural networks (Beurdeley et al., 2012; Frischknecht et al., 2012; Donato et al., 2013; Liu et al., 2013; Lensjø et al., 2017). Removal of PNNs reduces the activity of PV+ interneurons, ultimately creating

a state of higher excitation in the network (Lensjø et al., 2017b). Additionally, PNNs are thought to stabilize synaptic connections and protect neurons from oxidative stress (Cabungcal et al., 2013; Berretta et al, 2015).

1.3.1 PNNs in schizophrenia

The PNNs assemble when the central nervous system matures in the juvenile animal and normally stays relatively constant throughout life. In patients however, post mortem investigations indicate that the number and density of PNNs are greatly decreased in the amygdala, entorhinal cortex and prefrontal cortex in individuals with SCZ (Berretta et al., 2015). In prefrontal cortex, PNN densities showed a 70% reduction in schizophrenic subjects compared to controls (Mauney et al., 2013). In patients, it is not clear if these changes are a result of the PNNs failing to form or whether they are degraded without being regenerated in the adult, possibly caused by the use of medication. In a pharmacological rodent model of SZ, exposure to ketamine reduced mPFC PNN levels, leaving hippocampal PNN intact, suggesting region-specific sensitivity to drug exposure (Matuszko et al., 2017). Loss of PNNs has been found to alter the firing properties of PV+ cells (Favuzzi et al., 2017; Lensjø et al., 2017b), and malfunctioning inhibitory network is linked to SCZ (Lodge et al., 2009; Murray et al., 2015). Causal correlations between PNNs, inhibition and development of SCZ remain elusive however.

In SCZ, positive, negative and cognitive symptoms have been associated to failure in coordination of information processing between brain regions and have mostly been attributed to impairments in the prefrontal cortex. (Wolkin et al., 1992; Weinberger et al., 1996; Haig et al., 2000; Ford et al., 2002; Allen et al., 2012). Impairments related to mPFC are often associated with inhibitory circuits (Hanada et al., 1987; Benes et al., 1996; Lewis et al., 2005; Schmiedt et al., 2005; Basar-Eroglu et al., 2007). This is also likely for SCZ where GABAergic signaling and in particular PV+ cell activity, which regulates the output of excitatory pyramidal cells is responsible for oscillations in the gamma frequency range. Reduced gamma oscillations are as previously mentioned a hallmark of SCZ. (Perry et al., 1979; Benes and Berretta, 2001; Heckers et al., 2002; Benes et al., 2007; Uhlhaas et al., 2009)

1.4 Cre-Lox recombination

The advancements within genome-editing methods holds a potential to extensively increase our understanding of the pathophysiology of complex genetic diseases like SCZ. When studying human disease, like SCZ, it is important to choose an animal model with neural processes that are comparable to humans. Established mice models are readily available to study both PPI and selective PNN knockout in PV+ cells. Typically, injections the chondroitinase ABC (ChABC), a bacterial enzyme that degrades chondroitin 4-sulphate and chondroiting-6 sulphate, has been used for PNN degradation. However, because CSPGs are common in the ECM, ChABC will degrade more than just PNNs and therefore, a more precise method is needed with minimal off-target damage to the ECM and effects restricted to PV+ cells. In that regard, the Cre-Lox recombination system is an alternative method for targeted gene editing in live animals that can be used for selective PV+ cell associated PNN knockout (Lanton et al., 2015).

Cre-Lox recombination is a is used to perform site-specific DNA rearrangements. The technique depends on the tyrosine recombinase enzyme Cre to catalyze the recombination event between associated DNA recognition sequences called LoxP sites. Sandwiching of DNA between LoxP sites is known as floxing. The orientation of the LoxP sites is important because they determine the outcome of the recombination event that is catalyzed by Cre, whether this is a deletion, inversion or translocation of DNA segments (Figure 1.4).

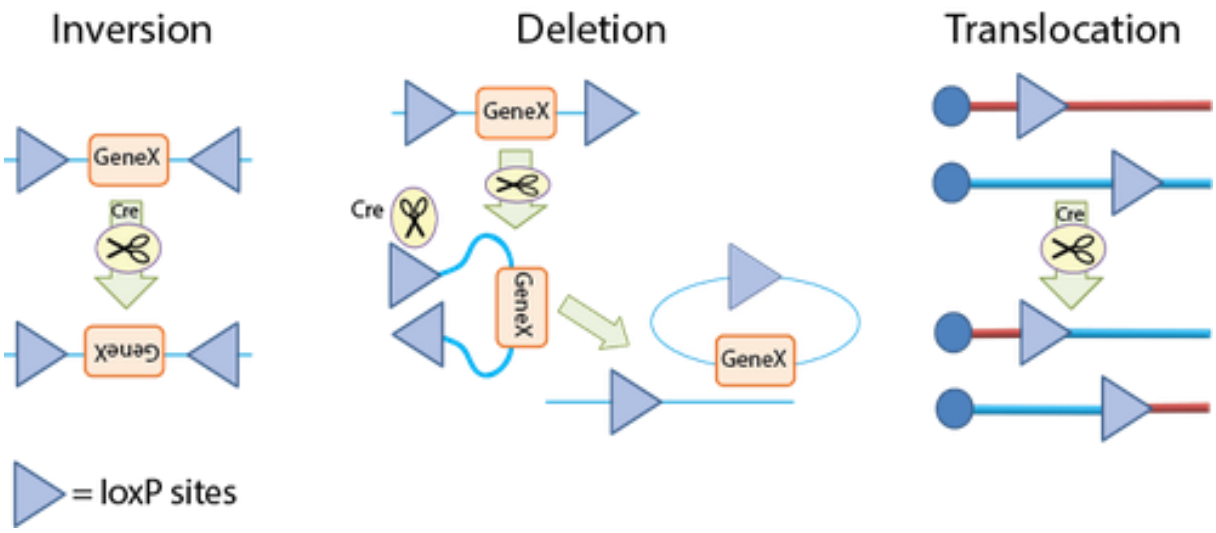

Figure 1.4: Cre-Lox recombination. The outcome Cre-Lox recombination is determined by the location and orientation of the flanking LoxP sites (triangles). (Left) Cre mediates the inversion of floxed DNA if the LoxP sites are arranged in opposite directions. (Middle) Cre cleaves the floxed DNA if the LoxP sites on the same chromosome are oriented in the same direction, producing a deletion. (Right) Cre catalyzes the chromosomal translocation of DNA if the LoxP sites are situated on different chromosomes. Figure from https//addgene.org/cre-lox/.

Expression of Cre can be put under the control of a general promoter for expression in an entire transgene animal. Alternatively, Cre can be placed under a tissue or cell-specific promoter for more contained expression (Fig 1.5). Different families of viruses can also be used to introduce Cre into a cell with a floxed gene, such as retroviruses, lentiviruses, adenoviruses and adeno-associated viruses (AAV). Moreover, Cre expression can be achieved using a modified form of Cre that is only functional when an inducing agent, such as Tamoxifen, is administered at the desired time (Garcia and Mills., 2002). Recombination events can therefore target specific brain areas and cell types; additionally, the investigator can choose the timing of recombination by using virus or Tamoxifen induced expression. This makes the Cre-Lox technology a powerful tool to study the role of a gene.

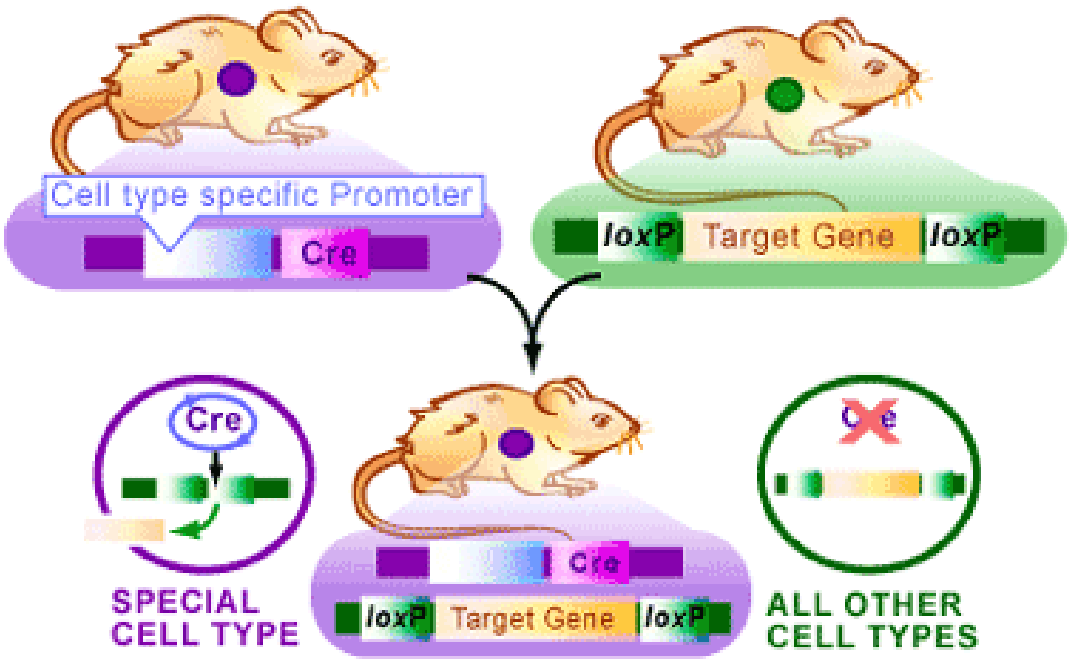

Figure 1.5 Cre-Lox mouse breeding: The knockout of a target gene in specific cell types by developing a Cre-Lox strain. Cre expression is placed under a cell type specific promoter in one of the parents, while the gene of interest has been floxed for deletion in the other. When crossed a cre-Lox strain is produced in which only target cells are subject to target gene knockout. Figure from http://www.scq.ubc.ca/targeting-your-dna-with-the-crelox-system/

1.5 Aims of this study

The main objective of this study is to examine whether perineuronal nets support prepulse inhibition of the acoustic startle reflex in mice, and whether PNNs in mPFC specifically are critical for normal PPI of the ASR.

In order to investigate the role of PNNs in PPI the following sub-goals were defined:

a) Establishing an experimental protocol to test PPI of the ASR in mice.

b) Is PNN presence across brain regions necessary for normal PPI? This was addressed by comparing the startle amplitude and PPI of mice with brain-wide PV+-cell specific aggrecan knock-out with control mice

c) Is PNN presence in the mPFC necessary for normal PPI? This was addressed by comparing the startle amplitude and PPI of mPFC virus-induced conditional knockout mice with viral control mice.

2. Materials and methods

2.1 Approvals and research animals

Laboratory work was done at the Department of Biosciences (IBV), Faculty of Mathematics and Natural Sciences (MN), the University of Oslo, Norway. All animal experiments were approved by the Norwegian Research Committee (FDU) and were performed in accordance with the Norwegian Animal Welfare Act and the European Convention for the protection of Vertebrate Animals used for Experiments and other Scientific purposes.

All personnel involved hold an animal research certificate (corresponding to a FELASA C course) and are approved by the FDU to conduct research experiments with animals.

Mice were housed in transparent polycarbonate cages (1290D Eurostandard type III, 42.5x26.6x15.5 cm, 820 cm^2 floor area) with woodchip bedding (Scanbur A/S, Karslunde, Denmark). The housing room temperature range was 21±0.1°C, humidity levels were at 55±10% and a ventilation rate of 5-20 times/hr. Mice were housed with a 12-hour day/12-hour night cycle (8AM to 8PM) with a light intensity of less than 100 lux during the day phase. Experiments were conducted during the day cycle (9AM-8PM). Food and water were available ad libitum. Animals were group housed. In cases where fighting was observed, animals were either single housed or housed in smaller groups as necessary.

2.2 Genotypes and experimental groups

Two strains of mice on a C67BL/6 genetic background were used for this study; G11 $ACAN^{-/-}$ and the G11 crossed to a PV-Cre mouse (ACAN/PV KO). C57BL/6 mice have been found to show average levels of acoustic startle reflex (ASR) and PPI among 40 inbred strains of mice (Willot, et al,. 2003).

Dr. Gunnar Dick (University of Oslo) developed the G11 mice in the laboratory of Professor James Fawcett (University of Cambridge, UK). In this strain, the 4^{th} exon of the ACAN gene is floxed (flanked by LoxP sites), allowing for conditional knockout of ACAN by Cre-Lox

recombination (Rowlands et al., in revision). The ACAN gene encodes the proteoglycan aggrecan, an essential core protein in the formation of perineuronal nets (PNNs). Tail biopsies were taken from offspring of locally bred G11 transgenic mice and analyzed by PCR and gene sequencing with forward and reverse primers to detect LoxP insertions for confirmation of genotype.

Aggrecan PV-knockouts are made by crossing PV-Cre and G11 mice. Homozygote crosses are born without the 4th exon of the ACAN gene in parvalbumin positive (PV+) neurons. Perineuronal net (PNN) development is dependent on the expression of aggrecan. Therefore, PNNs will never develop around PV+ neurons in this mouse line. The global loss of PNNs around PV+ cells in Aggrecan PV-knockout was confirmed by immunohistochemistry.

Heterozygous (HET) and homozygous (HOMO) G11 mice were split into three groups. The first consisted of HOMO G11 mice treated with AAV9.hSyn.HI.eGFP-Cre.WPRE.SV40 (University of Pennsylvania Vector Core, USA, from now on referred to as AAV9.eGFP-Cre). The second group contained HET G11 mice and were treated with AAV9.eGFP-Cre, this group retained PNN production with one wild type (WT) ACAN allele. The third group consisted of a mix of untreated HET and HOMO G11 mice.

The fourth experimental group consisted of the Aggrecan/PV+ knockouts. The different experimental groups of mice and their treatments prior to PPI experiments are listed in table 2.1.

Table 2.1: The four experimental groups. Group 1 and 2 received viral injections and express Cre-recombinase in transfected cells. Group 3 and 4 had no virus injection.

Group	Genotype	Viral injection	Aggrecan	PNN
1. Virus injected experimental group, n=7	G11 HOMO LoxP (G11 HOMO)	Yes	Not expressed in Cre-transduced cells	Lost around Cre-transduced cells
2. Virus injected controls, n=7	G11 Het LoxP (G11 HET)	Yes	Expressed	Maintained
3. Untreated controls, n=22	G11 HET & HOMO LoxP (G11 Untreated controls)	No	Expressed	Maintained
4. Global PV+ aggrecan knockouts, n=11	Global aAggrecan PV-Knockouts (ACAN/PV KO)	No	Not expressed in PV+ cells	Never produced around PV+ cells

2.3 Surgery and intracortical virus injections

Surgical instruments were cleaned and heat sterilized with a dry bead sterilizer (Germinator 500, CellPoint Scientific, Gaithsburg, MD, USA**)**. The surgery bench and the stereotaxic frame setup were cleaned thoroughly with water and 70% alcohol.

Mice were given intraperitoneal injections of a mixture of Ketalar (120 mg/kg ketamine) and Rompun (16 mg/kg Xylazine). Reflexes (tail tip and leg skin pinch) were carefully checked to assess the level of sedation. During surgery, the mouse was kept on a heating pad.

The animal was fixed to a stereotaxic frame using ear bars. The surface of the head was shaved and the exposed skin was cleaned with chlorhexidine. Eyes were lubricated with drops of viscotears (Théa Laboratories, Clermont-Ferrand, France) and a cardboard shield was placed over their eyes for additional prevention of light-induced retinal damage.

A longitudinal incision in the skin was made before membranes were removed with cotton swabs to access the cranium. Sterile saline water (0.9% NaCl) was regularly applied to the

skull to keep it moist. Bilateral craniotomies (+2.0 AP, ± 0.3 ML) were made above the mPFC using a dental drill.

Viral vector (AAV9.hSyn.HI.eGFP-Cre.WPRE.SV40, AV-9-PV1848, University of Pennsylvania Vector Core, USA) were bilaterally injected with a micro injector (Nanoject III, Drummund Scientific Company, PA, USA) mounted to the stereotaxic frame. Coordinates used for the injection in the prelimbic and infralimbic targets of the mPFC are listed in Table 2.2 and are based on coordinates from a mouse brain atlas (Paxinos and Franklin, 2001).

Table 2.2: The coordinates used for microinjection in prelimbic and infralimbic cortices of the mPFC. AP (anteriorposterior), ML (mediolateral), DV (dorsoventral). AP/ML coordinates measured relative to bregma, DV measured relative to dura

AP	ML	DV
+ 2.0	-0.3	- 2.5
+ 2.0	+ 0.3	- 2.5

The originals viral stock solution had a concentration of 10^{14} GC /mL (genome copies per ml) which was stored at -80˚C in many smaller aliquots. Aliquots were thawed on ice and diluted 1:10 with filtered 1X PBS to a concentration of 10^{13}GC, and immediately loaded into the micro pipette before surgery. Injections were done in four doses of 0.05nL to a total volume of 0.2nL in each hemisphere, with 20-second breaks between doses. The glass pipette was left in the tissue for 10 minutes after the last dose before being slowly retracted.

The incisions were sutured upon completing surgery, and mice were given subcutaneous injections of Rimadyl (5.0 mg/Kg Carprofen, analgesic), Antisedan (2.5 mg/Kg antisedative) as well as 0.5 mL saline for rehydration. Following surgery, mice were placed in a cage covered by a heating pad and monitored until normal behavior was reestablished.

Mice were given Rimadyl (5.0 mg/Kg) and Temgesic (0.15 mg/Kg) three days following surgery, with daily checkups for the next weeks. To ensure complete virus expression, PPI testing was delayed until5-6 weeks post-surgery.

2.4 Prepulse Inhibition

2.4.1 Equipment, software and calibration

Experiments were conducted using a prepulse inhibition (PPI) startle package for mice (Med-Associates Inc., Fairfax, VT, USA) with two testing stations (Figure 2.1). The package includes two sound attenuating cubicles (ENV-022S, interior 55.9x34.3x35.6 cm / exterior 63.5x41.9x39.4 cm), two small grid rod animal holders (6x6x4.8 cm), two PHM-255 stimulus connection panels with platform table and speakers, two PHM-250B Startle Load Cell Amplifiers, a startle reflex cabinet (with ANL-729, ANL-925E and ANL-925D), calibration package (ANL-929A-PC USB microphone package and load cell calibration weights), cables and software. The PHM-255 stimulus connection panel is comprised of a startle load cell for movement detection (measures downward force/weight) and two speakers with audio amplifiers. One of the speakers on each panel can produce background noise up to 100 dB sound pressure level (SPL) while the other generates short startle pulses up to 120 dB SPL with 1 ms rise/fall time. Animal holders were attached onto their respective stimulus connection panels (Figure 2.2).

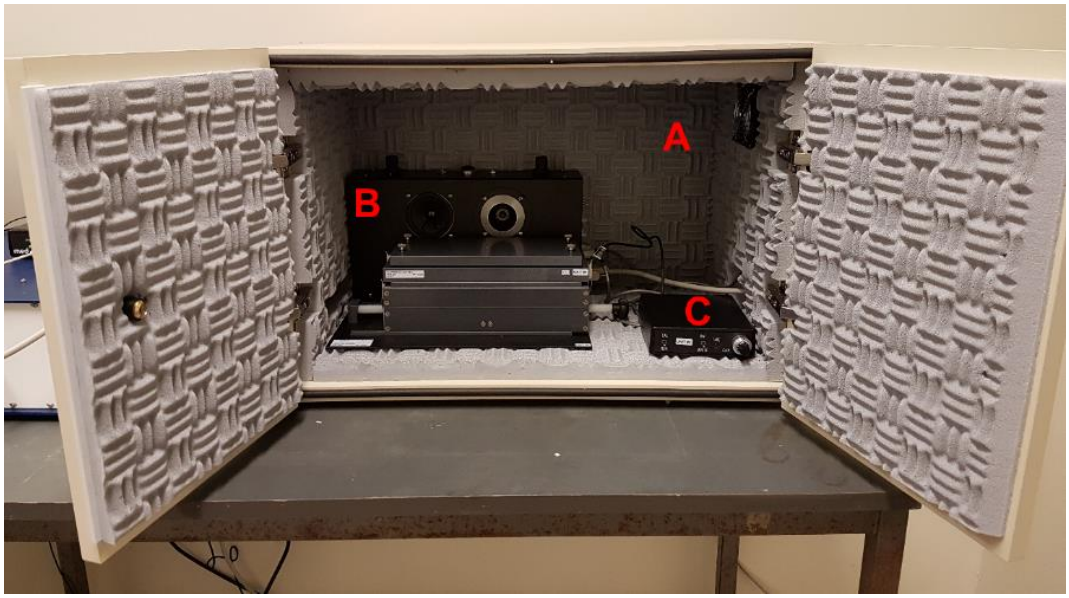

Figure 2.1 PPI test station: (A) Sound attenuating cubicle lined with sound isolating padded walls. (B) Stimulus connection panel with speakers and platform table with load cell. (C) Startle load cell amplifier.

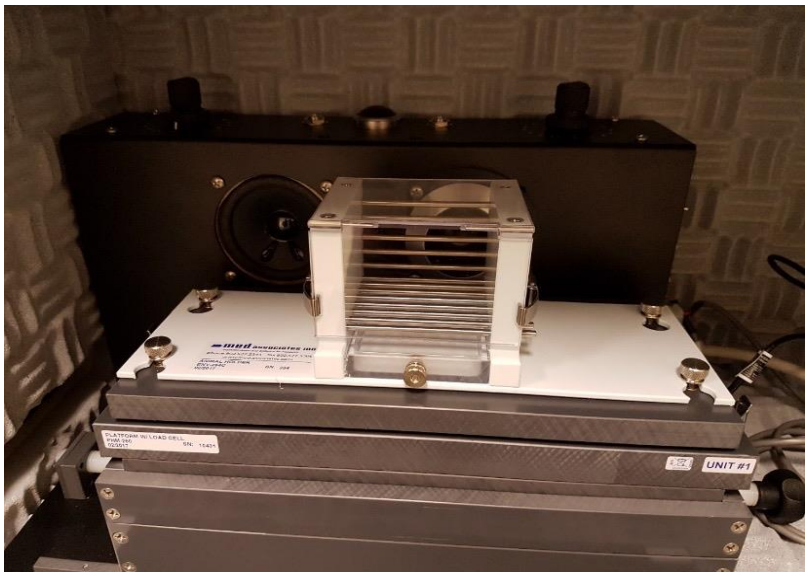

Figure 2.2. Placement of the animal holder on the stimulus connection panel: The animal holder (white) is fixed on the load cell platform in front of the speakers.

Accompanying software (Startle Reflex and sound calibration software) was run on a computer with one full-height PCI slot and Windows XP-32 bit (Microsoft Corporation, Redmond, WA, USA). The Startle Reflex software allows flexible programming to tailor PPI experiments within a customizable range.

The startle reflex package was designed to produce stimuli and collect response data for waveform analysis. The amplitude of the startle response is quantified by the startle load cell as an analog voltage signal between -10V and +10V, which is converted to a digital unit with a value between -2048 and 2048.

2.4.2 Calibration of sound and startle load cell

Equipment was calibrated according to manual with supplied hardware and software.

Audio was calibrated on both speakers with the USB microphone package and audio calibration software (Calibrate Audio function in Startle Reflex and ANL 929A Sound Level Meter). The speaker adjustment knobs above the speakers were also used to fine tune dB levels. Audio calibrations were done once per day before starting a daily round of experiments.

The load cell calibration was performed by adjusting the Tare (offset) and gain on the startle load cell amplifier in conjunction with the Calibrate Input function in Startle Reflex. To calibrate the load cell for mice, a 40g weight was placed inside the animal holder when adjusting the gain. The same standard weight was used to calibrate for all animals, irrespective of mass differences between mice. The load cell was calibrated before every experiment.

2.4.3 Single stimulus startle test

A single stimulus startle test was designed to assess how mice responded to sound stimuli at different sound pressure levels (SPL). The primary goal of the experiment was to ensure that prepulses chosen for PPI experiments did not exceed the startle threshold of the subjects. Additionally, the test was used to uncover abnormal startling behavior or hearing deficits in our test subjects. A constant background noise of 65 dB was present during the entire session. Mice were habituated to background noise for 5 minutes prior to testing. The experiment included sound stimuli between 70 dB and 120 dB with 5 dB increments, arbitrarily presented; individual sound pulses lasted 40 ms and was repeated four times throughout the test. In total, 44 sound pulses were presented in a pseudorandomized order with pseudorandomized intertrial intervals (ITI) of 10-20 seconds. Both sound stimuli and background noise were white noise.

2.4.4 Prepulse inhibition test

A PPI program was designed based on existing literature (Daenen et al., 2003; Willot et al., 2003; Ralph and Caine., 2005; Takashi., et al 2007; Baldan Ramsey et al; 2011; Valsamis and Schmid., 2011; Basavaraj and Yan., 2012; Ronca et al., 2017), with the aim to ensure that experiments were performed with optimal testing conditions. A wide series of testing parameters were evaluated and tried in a pilot phase, ranging from acclimation time, number of trials, trial duration and trial types, stimulus intensity, duration and rise/fall time, inter-stimulus and inter-trial duration. When selecting parameters, few trials with ideal stimulus range and intensity were selected to limit the duration of the testing sessions to ensure sufficient data per trial type.

The PPI experiment contained 80 trials in total and included four trial types:

1. Prepulse and startle pulse (S1 + S2). For assessing inhibited startle in PPI.
2. Prepulse alone (S1). To control for prepulse-induced startle.
3. Startle pulse alone (S2). For assessing maximum startle.
4. No stimulus (NOSTIM). Control for baseline movement.

Startle pulses were always 120 dB (white noise) while prepulses were either 68, 74 or 80 dB (white noise) (Figure 2.3). As is standard in the literature to reduce variability in testing, a constant background noise of 65 dB was present during the entire experiment.

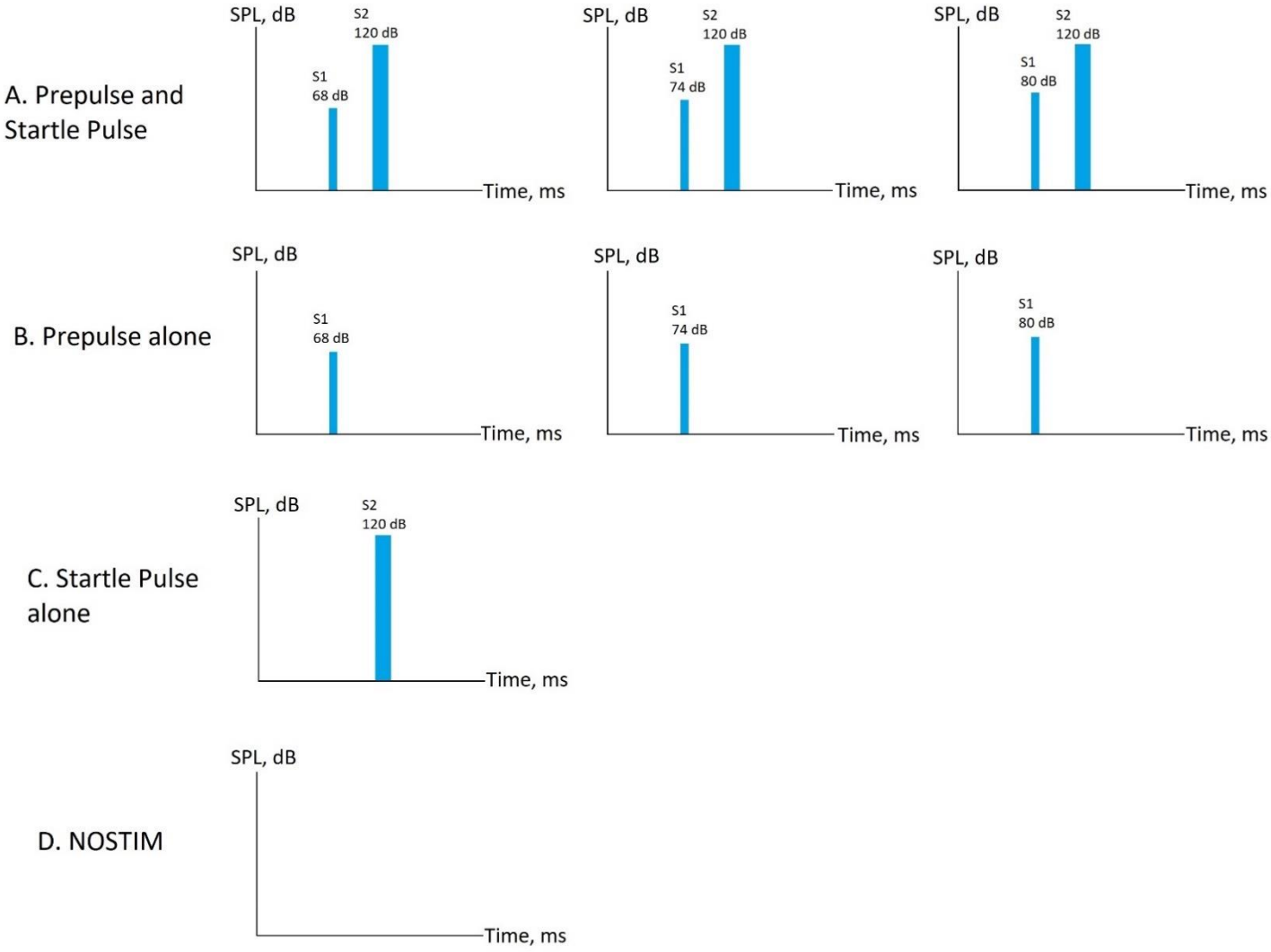

Figure 2.3: PPI experimental configuration. The PPI program contained four trial types, eight different subtypes, each presented 10 times in pseudorandomized order. (A) Prepulse coupled with startle pulse, three different prepulse levels. (B) Prepulse alone. (C) Startle pulse alone. (D) No stimulus.

Trial type A in the PPI experiment started with a null period of 200 ms followed by a 20 ms prepulse, 100 ms interstimulus interval (ISI), 40 ms startle pulse and a 160 ms post startle period. Total trial-time was 520 ms followed by a 10-20 second intertrial interval (ITI) before the next trial (Figure 2.4). Silence replaced the S1 and/or S2 interval in trail type B, C and D, but where otherwise equal to trial type A.

Movement recordings of the subjects were made during three phases: the null period, the S1 and ISI, and during S2 and the post startle period. Recorded peak responses to S2 in the post startle period were used for PPI data analysis. Multiple peaks follow a startle response, and the first peak value that satisfied built in inclusion criteria of 30 ms minimum latency, 50 minimum peak value and 30 ms minimum peak value, were registered. Trials were excluded if there was found excessive roaming movements during the null period or startle in response to S1 in the ISI period.

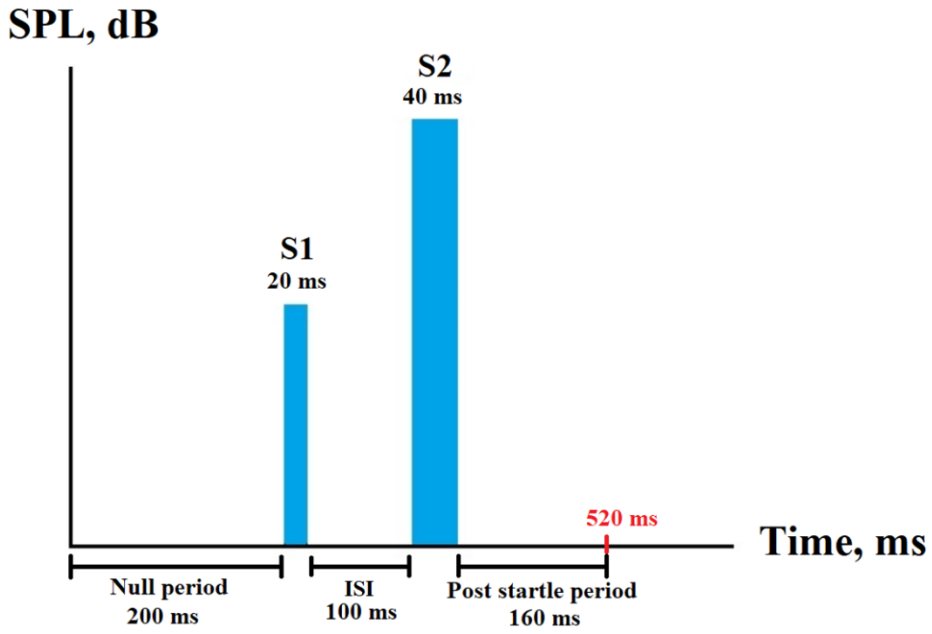

Figure 2.4: Time intervals, stimuli and recording. Trials started with a null period of 200 ms followed by a 20 ms prepulse, 100 ms interstimulus interval, 40 ms startle pulse and a 160 ms post startle period. Trials lasted for 520 ms and were followed by a 10-20 second break before the next trial. Silence replaced the S1 and/or S2 interval in trials without these pulses.

2.4.5 Experimental timeline

Viral vector injections were completed 5 or 6 weeks before behavioral experiments to ensure complete viral transfection. Mice were habituated to the experimenter in daily sessions of 5 minutes for two weeks. Habituation to the startle rig was done in short sessions of 10 minutes with only background noise (65 dB white noise) one week prior to startle experiments. The single stimulus startle tests were conducted first, followed by PPI the next two days (Figure 2.5).

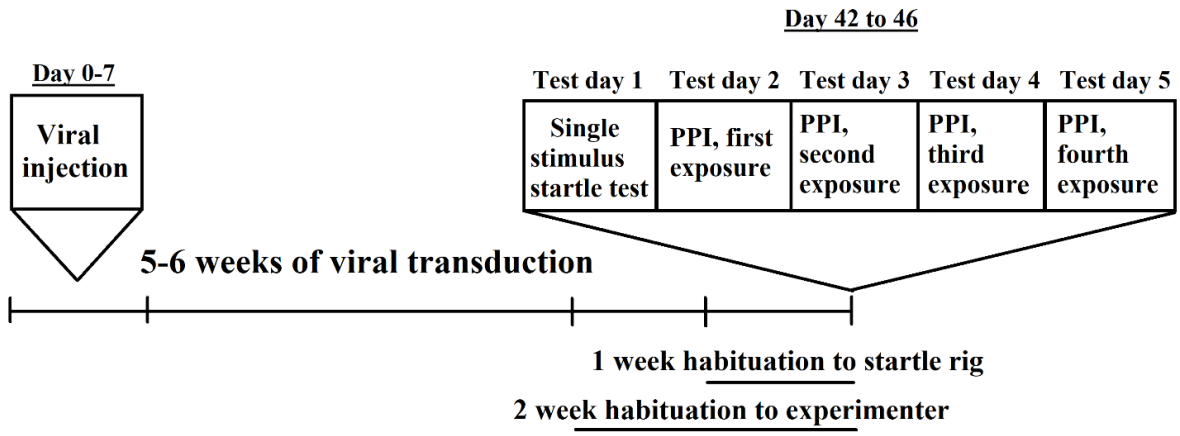

Figure 2.5: Timeline of procedures. Virus injected mice were allowed to recover for 5-6 weeks after following surgery before behavioral testing. All animals were habituated to the experimenter two weeks and to the startle rig one week before participating in experiments for three days in a row. One day of single stimulus testing was followed by two days of PPI testing.

2.5 Histology and immunohistochemistry

2.5.1 Perfusions and tissue sectioning

Perfusions took place no later than five days after PPI experiments were concluded. Animals were anesthetized in induction chambers with isoflurane and then injected intraperitoneally with an overdose of pentobarbital sodium (25 mg/kg). When no response to toe pinch or cornea touching were observed, anesthesia was considered deep enough for perfusion. Transcardial perfusions were done with 0.9% NaCl in 1M phosphate-buffered saline (PBS) followed by 4% paraformaldehyde (PFA) in 1X PBS for fixation.

Brains were stored in 4% PFA overnight for further fixation and then incubated three to four days at 4°C in 30% sucrose solution in 1X PBS to ensure cryoprotection by dehydrating the tissue before freezing. The brains were then flash frozen and cut into 40 µm thick coronal sections using a cryostat (Ortomedic, Lysaker, Norway). Sections were transferred into a solution of 1X PBS containing 0.02% sodium azide for immunohistochemistry staining.

2.5.2 Immunohistochemistry

Coronal sections were stained while free floating in solution.

PNNs were visualized using the biotin-conjugated *Wisteria Floribunda Agglutinin* (WFA-biotin, Sigma-Aldrich Chemie, Munich, Germany). In order to amplify the GFP signal in transduced cells, we included anti-GFP (ThermoFisher Scientific, Waltham, MA, USA) in the staining protocol. In addition, 4',6-diamidino-2-phenylindole (DAPI) was used to stain cell nuclei.

Sections were first washed 3 X five minutes with agitation in 1X phosphate-buffered saline (PBS) before incubation for one hour in a blocking solution (1% Bovine Serum Albumin (BSA, Sigma-Aldrich, USA), 0.3% tritonX-100 (Sigma-Aldrich, USA) in 1X PBS). They were then incubated with WFA-biotin (1:200) and primary chicken GFP antibody (1:2000) overnight at room temperature. The following day, sections were washed (3 X five minutes in 1 X PBS) and incubated in secondary antibodies alexa-488 anti-chicken (1:400, ThermoFisher Scientific, Waltham, MA, USA) and streptavidin alexa-594 (1:1000, ThermoFisher Scientific, Waltham, MA, USA) in 1X PBS for two hours. Following the incubation, sections were washed (3 X five minutes in 1 X PBS) before being mounted on Superfrost plus glass slides (Thermo Fischer Scientific, Oslo, Norway) and dried for an hour. Slides were rinsed in ddH_20 before 2 drops of DAPI Fluoromont-G® staining solution (0100-20, AH Diagnostics AS, Oslo, Norway) was applied and sections were secured with cover glasses.

Similarily, ACAN/PV KO sections were stained with rabbit anti-parvalbumin (Swant Inc, Marly, Switzerland) and secondary antibody alexa-594 donkey anti mouse. ACAN/PV KO sections were also stained with PNNs.

2.6 Image acquisition and statistical analysis

2.6.1 Image acquisition

Fluorochrome stained sections were analyzed with a fluorescent microscope (axioplan 2 microscope) rig with supplied hardware and software provided by Carl Zeiss AG (Oberkochen, Germany). Images were taken with axiocam HRZ camera and stitched together with the MosaiX function of the Axiovision software. Images were treated in photoshop CS6 (Adobe, San Jose, CA, USA). High-resolution confocal images (provided by Dr. Kristian K. Lensjø and Sverre Grødem) were acquired in a step-wise manner through the z-plane using a confocal microscope with a 60x objective and 2x digital zoom. The spacing between each step in the z-plane was 0.47 µm. A max projection through the entire z-stack was then generated using ImageJ.

2.6.2 Statistical analysis

Experimental data were automatically logged in Microsoft Access database (Microsoft Corporation, Redmond, WA, USA) and then manually sorted in Microsoft Excel. Statistical analysis was performed using IBM SPSS Statistics (v25.0, IMB Corp., Armonk, NY, USA). All data were assessed for both normal distribution and homogeneity of variance using the Shapiro-Wilk test and Levene's test respectively. If these assumptions were not violated, PPI and startle value data were analyzed using repeated measures ANOVA, with prepulse (dB level) and test day as within subjects variables, and group (either ACAN/PV KO vs. G11 untreated, or G11 HET CRE vs. G11 HOMO CRE) as the between subjects variable. Any violations of sphericity were corrected using the Greenhouse-Geisser method. In the case of non-normally distributed data, non-parametric analyses were performed using Mann-Whitney U tests for between subject comparisons, and Friedman test of differences among repeated measures for within subject comparisons. Post hoc analysis of significant within-subject main effects were carried out using Wilcoxon Signed Rank sum test. All non-parametric tests were corrected for multiple comparisons using the Holm-Bonferroni method (Holm, 1979). Graphical representations were created using Graphpad Prism 7 (Graphpad Software).

3. Results

3.1 Histology

3.1.1 Fluorescence microscopy

Inclusion criteria based on the accuracy and spread of the viral injection in the medial prefrontal cortex (mPFC) was applied before interpreting the behavioral results in the cortex of PNN loss in the intended target area. To be classified as a successful injection it had to be bilateral and most of the viral distribution had to stay within the range of 1 mm medio-laterally from the midline and between +1.54 and +2.1 mm anteriorly to bregma (Figure 3.1).

Of the 14 mice that underwent surgery, only one was excluded. However, coronal sections of all cohorts revealed that all mice had some degree of spread to off-target locations (Figure 3.1). In all subjects, the viral distribution followed the dorsoventral path of the needle from the surface to mPFC and to some degree anterior-posteriorly from the target area.

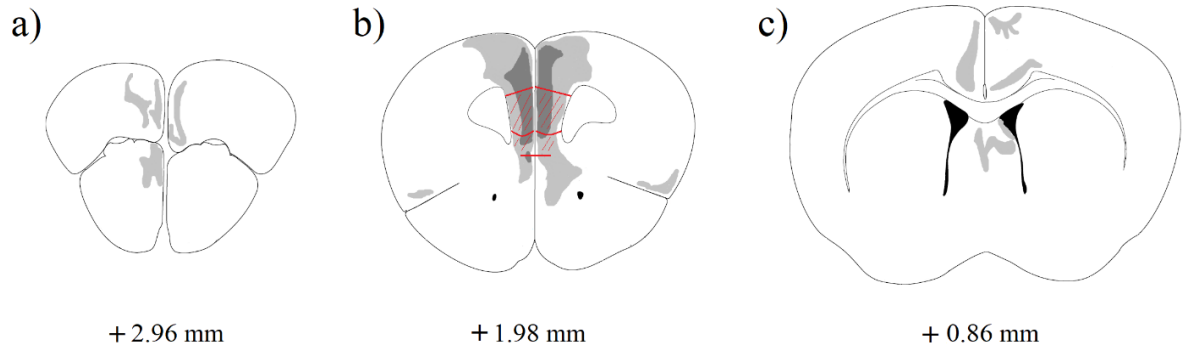

Figure 3.1: Schematic representation of adenovirus distribution after injection drawn on mouse atlas coronal sections. The illustrated coordinates of distribution in all three dimensions are based on visual estimates. Spread of virus on target anterior-posterior coordinates (b) and off target (a and c). Light gray represents the mouse with maximal spread of virus, anteriorly (a), posteriorly (c) or on target section (b). Dark gray (b) represents the injected mouse with the smallest viral spread. Red area with diagonal lines corresponds to the PrL and IL targets of the mPFC. Section coordinates distances anteriorly from bregma. Coronal sections modified from Paxinos and Franklin, 2001.

WFA staining of PNNs in G11 untreated controls demonstrates the normal levels and distribution of PNN expression in the adult mouse brain unaltered by manipulations (Figure 3.2a). While PNN levels were high towards the outer cortices, their numbers were naturally lower in the mPFC. As expected, the number of PNNs was dramatically lower in ACAN/PV KO than untreated G11 mice (Figure 3.2b). Sections from heterozygous (HET) and homozygous (HOMO) G11 viral injected cohorts revealed that PNN-breakdown by CRE expression depends on the floxing of both ACAN alleles. Expression of PNNs in CRE-expressing neurons were maintained in heterozygous (Figure 3.2c) but was lost in homozygous (Figure 3.2e) mice.

Upon further inspection by confocal microscopy, effects of genotype and viral exposure on PNNs was identified (Figure 3.3). In ACAN/PV KO mice, WFA signals did not overlap with PV signals (Figure 3.3b), demonstrating that the aggrecan gene had been successfully knocked out in PV+ cells. In the G11 HETs, CRE expressing mice maintained PNN production despite the loss of one ACAN allele (c), as is evident by the overlap of GFP and WFA signaling. On the other hand, transduced HOMO floxed mice were not found to express PNNs following double conditional knockout of ACAN (d). In the latter, no cells were found in which there was an overlap of GFP and WFA signaling and thus cells were either expressing GFP or PNNs.

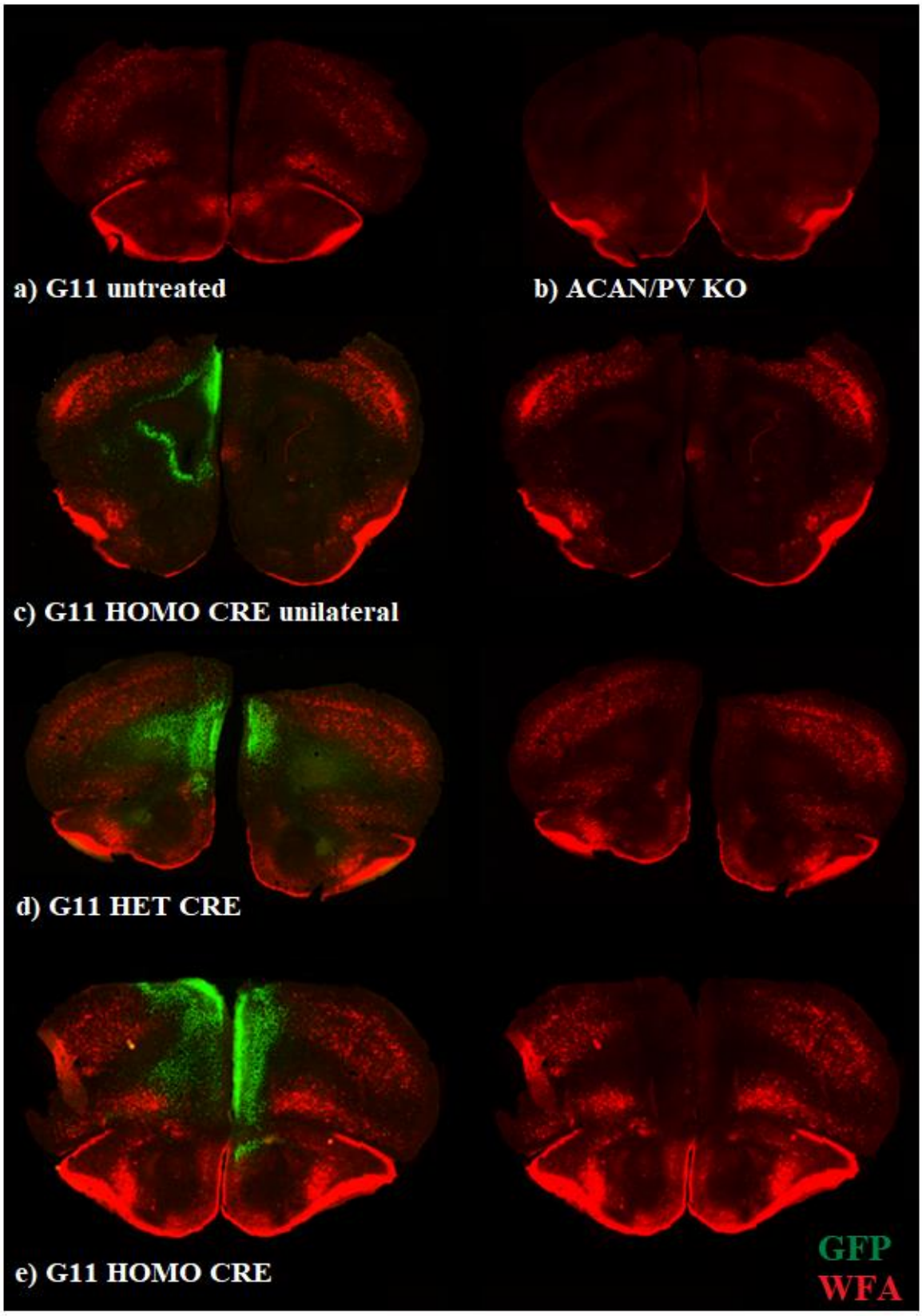

Figure 3.2: Coronal sections with virus distributions of the mPFC of mice. PNNs were stained with WFA (Red) and GFP transduction reporters with anti-GFP (green) in all sections. a) G11 untreated controls, (b) ACAN/PV KO, c) Unilateral injection of G11 HOMO CRE, d) G11 HET CRE, e) G11 HOMO CRE. Section coordinates approximately +1.98 mm anteriorly from bregma.

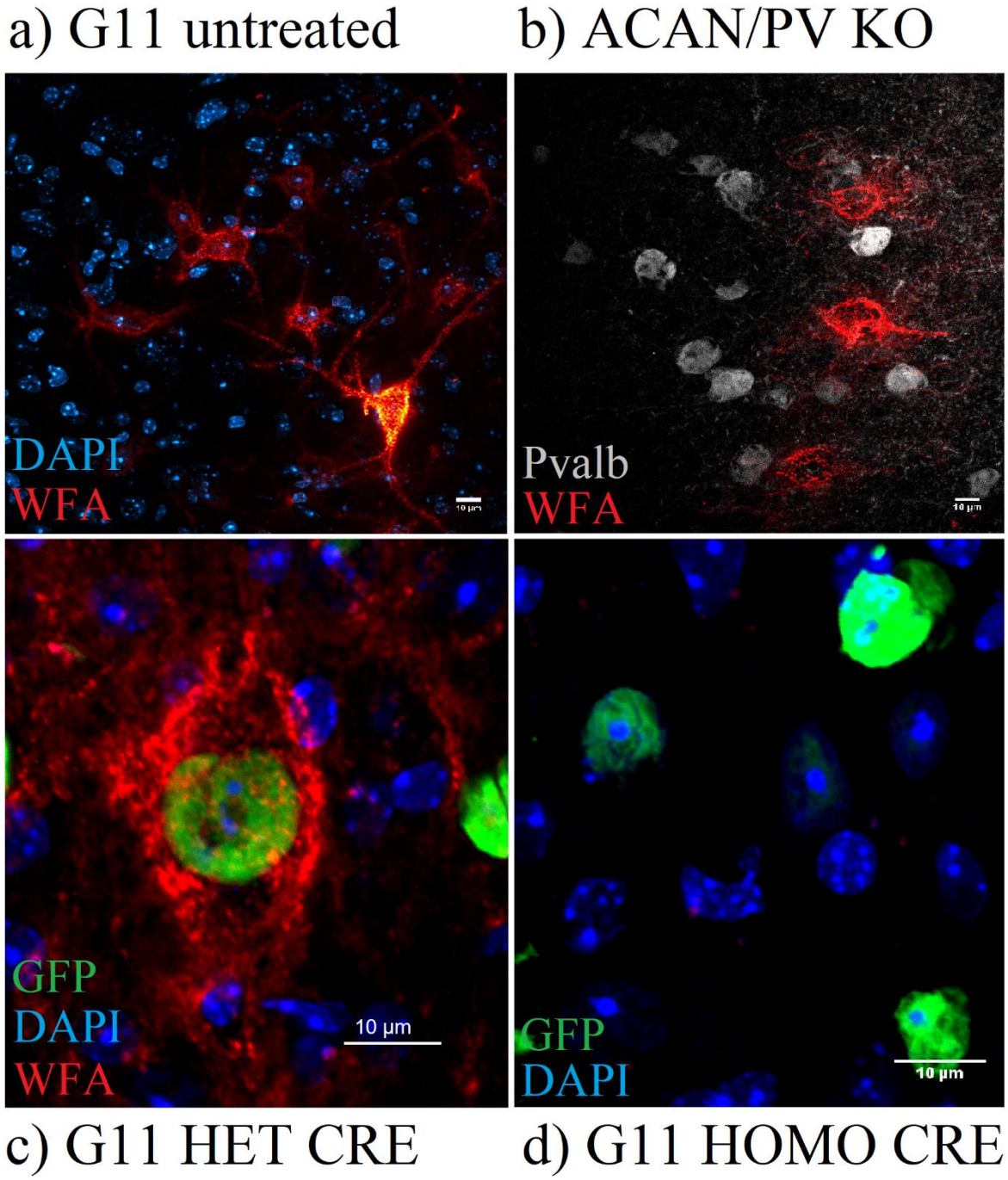

Figure 3.3 Deletion of Acan removes PNNs from PV+ cells. Z-stacked confocal images of G11 (a) and ACAN/PV KO (b) mice, and mice treated with virus injections (c,d). PNNs were stained with WFA (red), transduction reporter GFPs were stained with anti-GFP (green), nuclei were stained with DAPI (blue) and ACAN/PV KO with anti-PV (grey). (a) Heat map image of a G11 untreated control shows a brighter signal where the concentration of fluorochrome is highest. Individual PNN producing neurons are visualized as PNN enwrapped single nuclei. (b) PV and PNN staining does not overlap. c) Transduced G11 HET CRE neurons still maintain their PNNs. d) Transduced G11 HOMO CRE neurons do not maintain PNNs. (Scale bar 10 µm).

3.2 Single stimulus startle test

In response to single startle stimuli of 70-120dB intensity (5dB intervals; Figure 3.4), all groups had significantly higher startle amplitudes as a function of dB intensity (HOMO CRE: X^2 (6) = 34.939, $p < .0005$; HET CRE: X^2 (7) = 43.922, $p < .0005$; ACAN/PV KO: X^2 (11) = 77.240, $p < .0005$; G11 untreated: X^2 (22) = 119.810, $p < .0005$). Wilcoxon Signed rank test was carried out as post hoc analysis, comparing the 70dB startle amplitude data to all other dB data points. These comparisons revealed that all subsequent dB intensities were significantly higher than that obtained with the 70dB stimulus for the ACAN/PV KO and G11 untreated group (group difference comparison closest to p=.05: 70dB vs 75dB: $T(33) = 403.00$, $p < .05$), whilst in the HET CRE and HOMO CRE group, all comparisons with 70dB were significant with exception of the 70dB vs 75dB comparison (group difference comparison closest to the adjusted significance level: 70dB vs 80dB: $T(13) = 80.00$, $p < .05$).

In terms of group differences, visual inspection of Figure 3.4 suggests higher startle amplitude values for the ACAN/PV KO group compared to the other groups. Indeed, the startle amplitude of the ACAN/PV KO group was significantly higher than the G11 untreated group at 100dB, 110dB and 120dB stimulus intensity (100dB: $U(33) = 46$, $p < .005$; 110dB: $U(33) = 46$, $p < .005$; 120dB: 100db: $U(33) = 32$, $p < .0005$). The HET CRE startle amplitude values did not differ significantly from the HOMO CRE startle amplitude values. These results indicate that the startle response is affected by the global loss of PNNs around PV-cells, but the local removal of PNNs in mPFC had no impact.

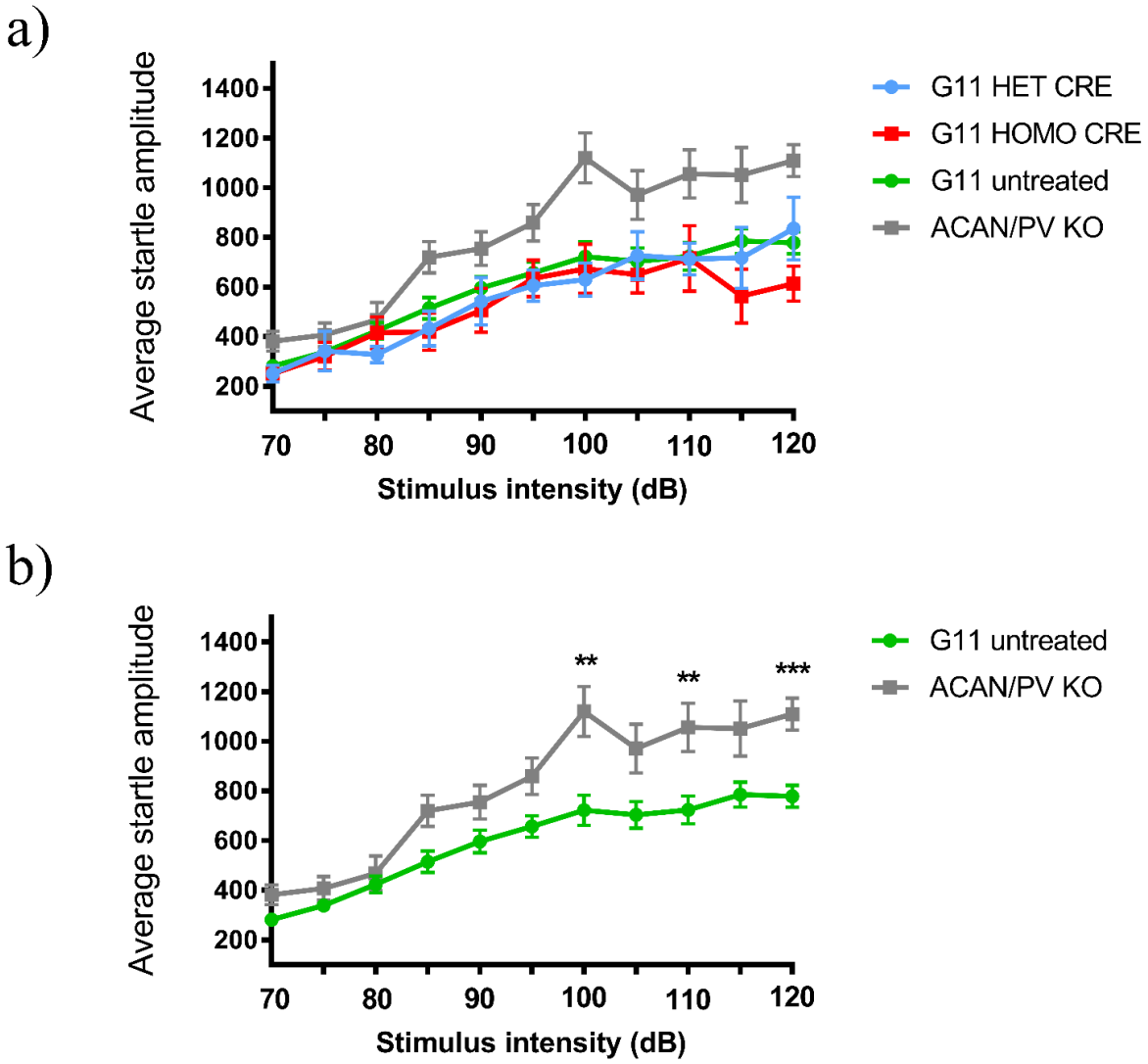

Figure 3.4: Single stimulus startle test. The mean startle response (amplitude) to a single stimulus startle test in the (a) non-injected groups of G11 untreated and ACAN/PV KO and the G11 untreated controls (green, n=22). G11 HET CRE expressing mice (blue, n=7), G11 HOMO CRE expressing mice (red, n=6) and ACAN/PV KO global ACAN knockouts (grey, n=11). (b) G11 untreated and ACAN/PV CRE data presented in isolation for clarity. ACAN/PV CRE mice had significantly higher startle amplitudes than controls (** = P < .005, *** = p <.001). Values are mean +/- standard error of the mean (SEM).

3.3. PPI of the ASR

Absolute PPI startle values between groups G11 HOMO CRE and HET CRE in response to 68+120, 74+120, 80+120 and 120 dB sound pulses revealed significance only when averaging data across test days 1-4 ($F(1,5)=7.334$, $p < .05$; Figure 3.5 a), but not when analyzing test day 1 in isolation ($F(1,11)= 2.595$, $p > .05$; Figure 3.5b).

Comparison between the G11 Untreated controls and ACAN/PV KO revealed that ACAN/PV KO mice had significantly higher PPI startle values compared to G11 untreated controls on all stimulus combinations when only analyzing test day 1 (group difference comparison closest to p=.05: 74 + 120 dB n = 33, U = 67, $p < .05$), but in only one stimulus combination when analysis across test days 1-4 (Startle Day 1, 120 DB: n = 33, U = 38, $p < .001$).

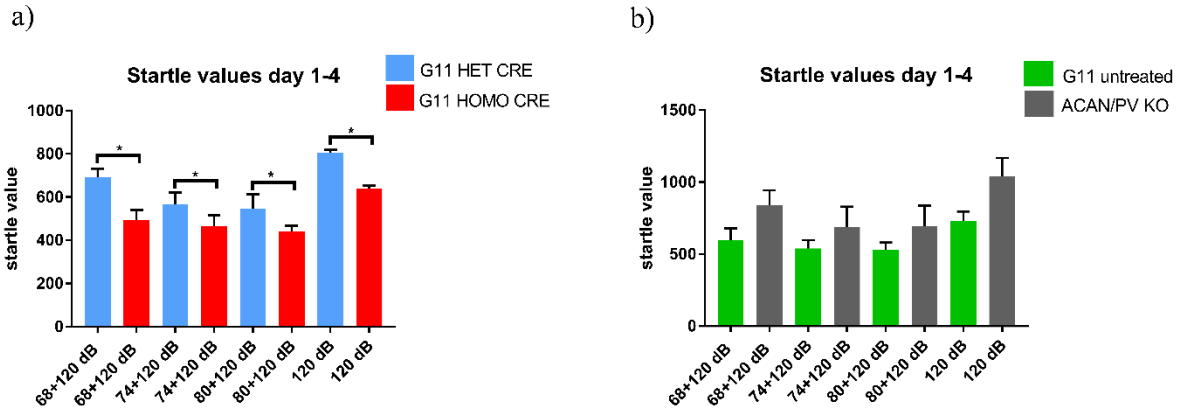

Figure 3.5: Absolute PPI. Mean startle amplitude values in the PPI of the ASR between (a) the surgery cohorts G11 HET CRE vs G11 HOMO CRE and (b) non-surgery cohorts G11 untreated controls vs ACAN/PV KO. G11 HET CRE had significantly higher startle values averaged across test days 1-4 than G11 HOMO CRE (* = $p < .05$). Values are mean +/-SEM.

No significant effects on PPI were found in any group in day 1 or across days 1-4 (Figure 3.6). This indicates that PNNs around PV+ cells, in the current experimental paradigm, are not essential for prepulse inhibition of the ASR.

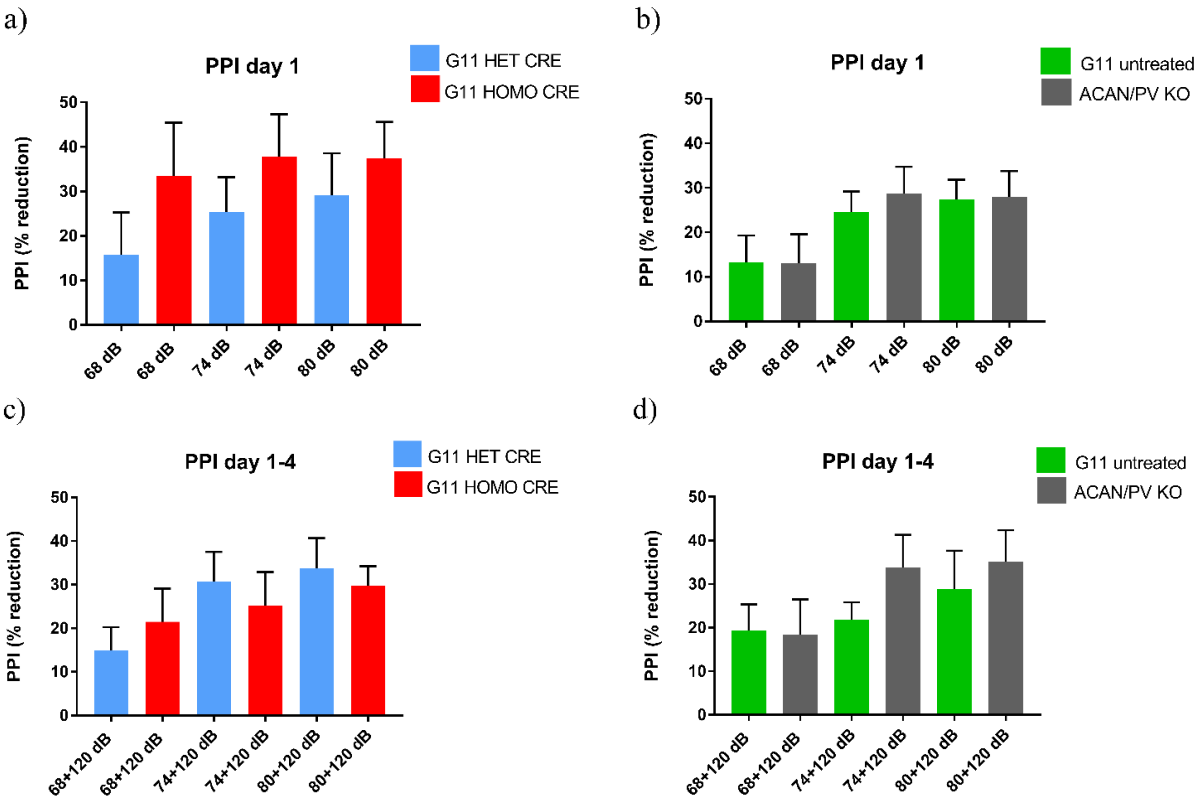

Figure 3.6: Relative PPI. PPI means in % of the ASR in (a) HET CRE and HOMO CRE on test day 1 only; (b) ACAN/PV CRE and controls on test day 1 only; (c) HET CRE and HOMO CRE on data averaged across test days 1-4; (d) ACAN/PV CRE and controls on data averaged across test days 1-4. There were no significant effect between groups. Values are mean +/-SEM.

4. Discussion

This study first examined if perineuronal nets (PNNs) are critical for PPI of the acoustic startle reflex (ASR), and second whether PNNs in the medial prefrontal cortex (mPFC) specifically contribute to normal PPI of the ASR.

It was found that ACAN/PV CRE mice have significantly higher startle amplitudes in response to single sound stimuli above startle threshold compared to G11 untreated mice, whereas G11 HET CRE mice did not show different startle responses compared to HOMO CRE. Moreover, absolute startle values during PPI testing were significantly different between G11 HOMO CRE and HET CRE while ACAN/PV KO and control animals showed similar values. However, when comparing the relative effect of the prepulse, that is, the degree to which the animals startled to the prepulse-startle pulse (S1+S2) relative to the degree to which they startled to the startle pulse alone (S2), there were no differences between groups.

While this experiment did not find an involvement of PNNs for PPI, the increased startle response to a specific stimulus in mice with a brain-wide knockout of PV+ cell associated PNNs indicates that PNNs may be important for normal development of sensory information processing. When PNN knockout was restricted to the mPFC of adults, the absolute startle amplitude in the PPI test was lower compared to controls, which might suggest that maintaining PNNs in the mPFC of adult mice is also important for normal sensory information processing. Why global loss of PNN expression compared to local loss of PNN expression in the mPFC affect different tests and why the effects are seemingly contradictory is open to speculation. Perhaps these findings can be attributed to a combination of the temporal aspect or location of PNN degradation. It is possible that removal of PNNs during development is more critical than during adulthood. This developmental effect could indicate how the observed lower levels of PNNs in schizophrenia patients may contribute to an imbalance in the excitatory/inhibitory network leading to distorted sensory information processing in these patients. Perhaps the altered startle response observed in ACAN/PV KO mice may be modified as an effect of a higher systematic aberration linked to PV+ impairments, like abnormalities in stress and cognition behavior.

In contrast to our experiments, PPI impairments were observed in in rats treated with chABC to degrade the PNNs in mPFC (Howland et al., 2016). The enzyme chABC digests chondroitin sulfate proteoglycans (CSPGs), thus degrading all extracellular matrix (ECM) containing CSPGs, not restricted to the PNNs. In that regard, our method with deletion of the gene for aggrecan is more targeted as the genetic knockout cause a selective degradation of the PNNs. Therefore, we can be confident that we have tested the effects of PNN removal on PPI and not extracellular matrix in general. Different sources may have caused the contradictory results between our experiments and Howland and co-workers such as:

(a) differences in how the PPI experiments were conducted and which could not be understood from the methods description, (b) differences between rats and mice, (c) differences in how much of mPFC that were affected by the treatment, (d) PV+ cells in the mPFC may be involved in PPI and that their activity relies on a more general integrity of the ECM, (e) perhaps other cells that may be affected by the chABC treatment but not the specific genetic knockdown in the mPFC are crucial to support normal levels of PPI. Further testing with larger group sizes and a direct comparison between chABC treatment and the genetic manipulation are necessary to understand the differences in the involvement of PNNs in mPFC for PPI.

Post mortem inspection from SCZ patients have found reduced levels of PNNs in the mPFC (Mauney et al., 2013; Berretta et al., 2015), but it is still unclear whether this lack of PNNs has any effect on brain function and behavior. One possible indication is the reduced inhibitory activity in SZC patients which may correlate to the reduced inhibitory activity after PNN removal in animal studies. The reduced inhibition in animal experiments is likely related to reduced PV+ cell activity. However, because these are separate findings, the effect of PNN removal on brain function are not conclusive. Our findings indicate that PNNs surrounding PV+ cells in the mPFC or elsewhere in the brain does not alter PPI. Nevertheless, PNNs are negatively charged and removal of these structures may affect the membrane potential and especially the ionic distribution along the membrane, and these distortions may affect normal firing activity of PV+ cells. The single startle pulse test revealed that PNNs are involved in mechanisms of sensory adaptation to sound stimuli in the audible range of the experiment, especially for stimuli above the startle threshold. However, the increased startle response was only apparent in the global aggrecan knockout mice, who are born without a functional ACAN gene and therefore fail to form PNNs during brain maturation. How ACAN knockdown influences PV+ cell activity is not known but it has been shown that removal of PNNs lead to reduced inhibitory activity, likely through reducing the activity of fast spiking PV+ cells. Reduced PV+ cell activity is a hallmark of immature neural networks during periods when there is heightened activity-dependent plasticity. (Hensch, 2005; Lensjø et al, 2017., Donato et al, 2013). It is not known how impaired PV+ cell function alters the startle response specifically but given is central role in information in feedforward and feedback inhibition of gamma frequency oscillations (Favuzzi et al., 2017; Lensjø et al., 2017b) it is likely that it will also influence sensory processing of the starte reflex.

4.1 Methodological considerations

The widely used PPI method provides a reliable, translational task with a clear phenotype in SCZ patients (Swerdlow et al., 2017). The task is robust to animal behavior such as orientation or posture when generating sound as stimuli. Despite this, some shortcomings were identified as probable sources of error. Experiments were conducted with closed cabinet doors to spare mice from distractions that would affect results, but as a consequence control over the emotional state and behavior of animals being tested is reduced. This includes stress related behavior that would be transduced by the load cell, such as running and jumping

during trials that would be mistaken as startle pulse-induced startle behavior. Most of this uncertainty was eliminated by built in exclusion criteria (latency time, startle time and amplitude), control trials and recording movement in the null time and inter-stimulus intervals to improve monitoring of behavior. It is advisable to improve control over behavior by installing cameras in the cubicles, as PPI is highly modulated by stress and the emotional state of the animal cannot be guaranteed even if great care is invested in habituation animals to experimenters and the test station.

Removal of PNNs from the mPFC was performed using intracranial injections of viral vectors. Risk of cortical damage is always associated with intracranial injections. To minimize the risk of damage, thin micro needles that in previous experiments have been shown to be suitable for such injections were used to avoid damage to the tissue (Thompson et al., et al 2017). Leaking of the virus along the tract of the syringe may result in less spreading of the virus or infection in overlying cortical areas. Low injection rates and leaving the syringe in the tissue to encourage diffusion of the virus distally from the infusion site prior to retraction were implemented to avoid this. A stereotaxic frame and the same coordinates were used on all animals to ensure optimal precision. Additionally, coordinates were re-measured after drilling to control for mis-positioning of the skull induced by the drill. Importantly, no behavioral comparisons were carried out between groups that differed in their exposure to surgery, and behavioral effects cannot therefore be attributed to surgical factors such as cortical damage or anesthesia exposure.

The Cre-Lox system was used for PNN-breakdown, creating a specific removal of PNNs in all transfected neurons expressing aggrecan. The effect was contained to neurons because Cre was put under a neuron-specific promoter (synapsin). Immunohistochemistry revealed that viral transductions lead to the loss of PNNs in HOMO CRE, but not in HET CRE mice. Despite confirmed loss of PNNs in all HOMO CRE mice, it is possible that the degree of viral infection, and subsequent PNN loss, differed in individual mice. This could contribute to the relatively high degree of inter-subject variability in startle amplitude measures, which could mask potential group effects. To counteract this, data from all four test days was analyzed, allowing for increased number of data points and reducing the effect of individual variability. Furthermore, a significant difference between HOMO CRE and control values was observed, suggesting that any potential differences in viral infection did not affect behavioral data to the extent that behavioral differences could not be established.

The effects of having only one ACAN allele on PNN size and expression threshold is not known. Potentially this could be a confounding factor that has been taken into consideration when assessing our findings. To avoid this problem in the future, the effects of Cre expression-inducing AAV injections versus control AAV injections can be compared between two respective homozygous ACAN floxed G11 groups.

The mPFC is an ideal target in which SCZ pathophysiology and part of the neural circuitry responsible for PPI overlap, but is only a part of the large-interconnected circuitry described to be involved in PPI. ACAN/PV KO mice were introduced to assess if the widespread knockout of PV+ cell associated PNNs were involved in that regard, but other targets aside

from the mPFC can be singled out for PNN degradation, such as the nucleus accumbens which has been identified as a crucial structure in the regulation of PPI (Swerdlow et al., 2016).

Mouse strains vary in their suitability to PPI testing due to genetic differences in auditory functioning and baseline levels of PPI (Paylor and Crawley., 1997). C57BL/6 mice were carefully selected for our study because they have been previously reported middle responders of PPI (Willot et al., 2003), have suitable hearing (Paylor and Crawley., 1997) and because there is an established animal strain for Cre-Lox ACAN knockout (Lanton., 2015).

4.3 Future perspectives

The results of this study need to be complemented by further work to determine whether the potential shortcomings in its design are important and further build on current findings. The G11 HOMO and HET groups were small and as a consequence compromising statistical power for these groups. In light of this, future experiments should be conducted with larger cohorts of mice. Additionally, a proposed solution for removing doubt whether G11 HET CRE undergo partial PNN degradation or elevated threshold for PNN expression and how this affects the data is: (a) to assess the HET CRE group alongside a wild type mouse (for a normal behavioral baseline reading), (b) compare G11 HOMO CRE group with cre-induced PNN knockdown and a G11 HOMO CRE group with AVV injections that do not induce Cre expression. Furthermore, reported findings of PPI impairments induced by ChABC in mPFC in rats should to be repeated in mice to see if effects are replicable, and compared to ACAN knockout mice to see if there are significant differences.

The outcomes of our experiments also open possibilities to investigate new questions. ACAN/PV knockout mice can be compared to adult, onset Cre-induced aggrecan knockout with dexocycline feeding system (Le et al., 2008), to disclose whether the abnormal sensory adaptation to stimuli is due to the absence of PNNs during development. Moreover, PV+ cells in the mPFC or elsewhere in the brain may retain sufficient activity without PNNs to support PPI despite the knockout or conditional knockout of PNNs; either because the contribution of PNNs is negligible or because of compensatory adaptation to retain stability. A possible solution is to investigate PV+ cell involvement in the mPFC with optogenetics as a tool to alter PV+ cell activity and asses if there are significant effect on PPI (Scudder et al., 2018), or alternatively by designer drugs exclusively activated by designed drugs (DREADDs) (Morrison er al., 2016). Lastly, the involvement of PNNs in other regions of the brain described as part of the PPI circuitry could be evaluated. We propose the nucleus accumbens as an ideal target, as it has been the main area of focus when mapping the neural circuitry responsible for PPI.

4.4 Conclusion

This study found that extracellular matrix structures known as PNNs influence the startle response to single sound stimuli in mice. Mice with brain-wide knockout of PNNs showed significant elevated levels of startle response compared to controls, possibly as a result of dysfunctional inhibitory circuitry due to the failure to express PNNs during maturation of the sensory processing systems. Whereas local knockout of PNNs show significant reductions in absolute startle response during PPI testing. PNNs were not found to be critically involved in PPI despite previous reports of impairment following PNN degradation with chondroitinase ABC in the mPFC, possibly due to different methodological approaches or species differences. The general of the ECM of the mPFC might therefore be critical for retaining normal levels of PPI but targeting PNNs specifically has no effect.

PV+ cells might still be important for retaining normal sensorimotor gating; however, it is unclear whether PNN degradation significantly destabilize their functional properties to affect PPI. Future studies utilizing methods like optogenetic to manipulate PV+ cell activity are needed to assess whether PV+ cells are involved in PPI. Additionally, the adult onset of global Cre-induced aggrecan knockout could dissect whether failure to develop PNNs in development or failure to maintain PNNs in adulthood is more important in regulating startle responses to abrupt, loud sound stimuli.

These findings provide further insight into the role of PNNs and their involvements in abnormal sensory adaptation to stimuli in SCZ.

5. References

Allen, P., Luigjes, J., Howes, O. D., Egerton, A., Hirao, K., Valli, I., Kambeitz, J., Fusar-Poli, O., Broome, M., McGuire, O. (2012). Transition to psychosis associated with prefrontal and subcortical dysfunction in ultra high-risk individuals. *Schizophr Bull* 38(6):1268–1276 https://doi.org/10.1093/schbul/sbr194

Baker, K. D., Gray, A. R., Richardson, Rick. (2017). The development of perineuronal nets around parvalbumin GABAergic neurons in the medial prefrontal cortex and basolateral amygdala of rats.

Baldan Ramsey, L. C., Xu, M., Wood, N., Pittenger, C. (2011). *Lesions in the dorsomedial striatum disrupts prepulse inhibition. Neuroscience 180*:222-8 https://doi.org/10.1016/j.neuroscience.2011.01.041

Balmer, T. S., Carles, V. M., Frisch, J. L., & Nick, T. A. (2009). Modulation of perineuronal nets and parvalbumin with developmental song learning. The Journal of Neuroscience, 19(41), 12878-85. https://doi.org/10.1523/JNEUROSCI.2974-09.2009

Balmer, T.S. (2016). Perineuronal nets enhance the excitability of fast spiking neurons. eNeuro 3(4) ENEURO.0112-16 https://doi.org/10.1523/ENEURO.0112-16.2016

Bartos M., Vida I., Frotscher M., Meyer A., Monyer H., Geiger JR., Jonas P. (2002) Fast synaptic inhibition promotes synchronized gamma oscillations in hippocampal interneuron networks. Proc Natl Acad Sci U S A. 99(20):13222–13227 https://doi.org/10.1073/pnas.192233099

Bartos M., Vida I., Jonas P. (2007) Synaptic mechanisms of synchronized gamma oscillations in inhibitory interneuron networks. Nat Rev Neurosci. (1):45–56 https://doi.org/10.1038/nrn2044

Basavaraj, S., Yan Jun. (2012). *Prepulse inhibition of acoustic startle reflex as a function of the frequency difference between prepulse and background sounds in mice. PloS One 7*(9):e45123 https://doi.org/10.1371/journal.pone.0045123

Benes FM, Berretta S. (2001). GABAergic interneurons: Implications for understanding schizophrenia and bipolar disorder. Neuropsychopharmacology. (1):1–27 https://doi.org/10.1016/S0893-133X(01)00225-1

Benes, F. M., Vincent, S. L., Marie, A. & Khan, Y. (1996). Up-regulation of GABAA receptor binding on neurons of the prefrontal cortex in schizophrenic subjects. *Neuroscience* 75, 1021–1031 https://doi.org/10.1016/0306-4522(96)00328-4

Benes FM., Lim B., Matzilevich D., Walsh JP., Subburaju S., Minns M. (2007). Regulation of the GABA cell phenotype in hippocampus of schizophrenics and bipolars. Proceedings of the National Academy of Sciences of the United States of America 104(24):10164–10169 https://doi.org/10.1073/pnas.0703806104

Berretta, S. (2012). Extracellular matrix abnormalities in schizophrenia. Neuropharmacology 62, 1584-1597. https://doi.org/10.1016/j.neuropharm.2011.08.010

Berretta S., Pantazopoulouos H., Markota M., Brown C., Batzianouli, E. T. (2015)- Losing the sugar coating: potential impact of perineuronal net abnormalities on interneurons in schizophrenia. Schizophr Res 167(1-3), 18-27. https://doi.org/10.1016/j.schres.2014.12.040

Beurdeley, M., Spatazza, J., Lee, H, H., Sugiyama, S., Bernard, C., Di Nardo, A, A., Hensch, T, K., Prochiantz, A. (2012). Otx2 binding to perineuronal nets persistently regulates plasticity in the mature visual cortex. J Neurosci 32:9429-9437. https://doi.org/10.1523/JNEUROSCI.0394-12.2012

Braff, D. L., Geyer, A. M. (1990). Sensorimotor gating and schizophrenia human and animal studies. Arch Gen Psychiatry 47(2):181-188 https://doi.org/10.1001/archpsyc.1990.01810140081011

Braff, D. L., Geyer, M. A., Light, G. A., Sprock, J., Perry, W., Cadenhead, K. S., Swerdlow. (2001). Impact of prepulse characteristic on the detection of sensorimotor gating deficits in schizophrenia. *Schizophr Res 49*(1-2):171-8. https://doi.org/10.1016/S0920-9964(00)00139-0

Braff, D., L. (2010). Prepulse inhibition of the Startle Reflex: A window on the brain in schizophrenia. *Behavioral Neurobiology of Schizophrenia and Its Treatment* 349-371. https://doi.org/10.1007/7854_2010_61

Burgess, H. A., Granato, M. (2007). Sensorimotor gating in larval zebrafish. J Neurosci 27(18):4984-94 https://doi.org/10.1523/JNEUROSCI.0615-07.2007

Buzsaki G., Leung LW., Vanderwolf CH. (1983). Cellular bases of hippocampal EEG in the behaving rat. Brain Res. 287(2):139–171 http://dx.doi.org/10.1016/0165-0173(83)90037-1

Cabungcal, J.-H., Steullet, P., Morishita, H., Kraftsik, R., Cuenod, M., Hensch, T. K., & Do, K. Q. (2013). Perineuronal nets protect fast-spiking interneurons against oxidative stress. Proceedings of the National Academy of Sciences of the United States of America, 110(22), 9130–5. https://doi.org/10.1073/pnas.1300454110

Cadenhead, K. S., Geyer, M. A., Braff, D. L. (1993). Impaired startle prepulse inhibition and habituation in patients with schizotypal personality disorder. *Am J Psychiatry 150*(12):1862-7. https://doi.org/10.1176/ajp.150.12.1862

Carstens, K. E., Phillips, M. L., Pozzo-Miller, L., Weinberg, R. J., & Dudek, S. M. (2016). Perineuronal Nets Suppress Plasticity of Excitatory Synapses on CA2 Pyramidal Neurons. The Journal of Neuroscience : The Official Journal of the Society for Neuroscience, 36(23), 6312–20. https://doi.org/10.1523/JNEUROSCI.0245-16.2016

Carulli, D., Rhodes, K. E., Brown, D. J., Bonnert, T. P., Pollack, S. J., Oliver, K., … Fawcett, J. W. (2006). Composition of perineuronal nets in the adult rat cerebellum and the cellular origin of their components. The Journal of Comparative Neurology, 494(4), 559–77. https://doi.org/10.1002/cne.20822,

Caeser, M., Ostwald, J., Pilz, P. K. D., 1989. Startle responses measured in muscles innervated by facial and trigeminal nerves show common modulation. *Behavioral Neuroscience, 103*(5), 1075-1081. http://psycnet.apa.org/doi/10.1037/0735-7044.103.5.1075

Celio, M.R., 1986. Parvalbumin in most gamma-aminobutyric acid-containing neurons of the rat cerebral cortex. Science (New York, N.Y), 231(4741), 995-7. https://doi.org/10.1126/science.3945815

Daenen, E. W., Wolterink, G., Van Der Heyden, J. A., Kruse, C. G., Van Ree, J. M. (2003). *Neonatal lesions in the amygdala or ventral hippocampus disrupt prepulse inhibition of the acoustic startle response; implications for an animal model of neurodevelopmental disorders like schizophrenia. Eur Neuropsychopharmacology 13*(3):187-97 https://doi.org/10.1016/S0924-977X(03)00007-5

Davis, M., 1980. Neurochemical modulation of sensory-motor reactivity: acoustic and tactile startle reflexes. Neuroscience & Behavioral Reviews, Vol 4, 241-263.

Davis, M., Walker, D., L., 1997. Amygdala and bed nucleus of the stria terminalis: differential roles in fear and anxiety measured with the acoustic reflex. Philos Trans R. Soc. Lond. B, Biol Sci, 352, 1675-1687 https://dx.doi.org/10.1098%2Frstb.1997.0149

Deepa, S. S., Carulli, D., Galtrey, C., Rhodes, K., Fukuda, J., Mikami, T., Sugahara, K., Fawcett, J. W., 2006. Composition of perineuronal net extracellular matrix in rat brain: a different disaccharide composition for the net-associated proteoglycans. The Journal of Biological Chemistry 281, 17789-800. https://doi.org/10.1074/jbc.M600544200

Delawalla, Z., Csemansky, J. G., Barch, D. M. (2008). Prefrontal cortex function in nonpsychotic siblings of individuals with schizophrenia. Biol Psychiatry 63(5), 490-7. https://doi.org/10.1016/j.biopsych.2007.05.007

Dityatev, A., Brückner, G., Dityateva, G., Grosche, J., Kleene, R., Schachner, M., 2007. Activity-dependent formation and functions of chondroitin sulfate-rich extracellular matrix of perineuronal nets. Develpomental Neurobiology, 67(5), 570-88. https://doi.org/10.1002/dneu.20361

Donato F., Rompani S, B., Caroni, P. (2013). Parvalbumin-expressing basket-cell network plasticity induced by experience regulates adult learning. *Nature 504*:272-276. https://doi.org/10.1038/nature12866

Ethridge, L. E., White, S. P., Mosconi, M. W., Wang, J., Byerly, M. J., Sweeney, J. A. (2016). Reduced habituation of auditory evoked potentials indicate cortical hyper-excitability in Fragile X Syndrome. *Transl. Psychiatry* 6:e787. https://doi.org/10.1038/tp.2016.48

Favuzzi, E., Marques-Smith, A., Deogracias, R., Winterflood, C. M., Sánchez-Aguilera, A., Mantoan, L., … Rico, B. (2017). Activity-Dependent Gating of Parvalbumin Interneuron Function by the Perineuronal Net Protein Brevican. Neuron, 95(3), 639–655.e10. https://doi.org/10.1016/J.NEURON.2017.06.028

Ford J. M., Mathalon, D. H., Whitfield, S, Faustman, W. O., Roth, W. T.. (2002). Reduced communication between frontal and temporal lobes during talking in schizophrenia. Biol Psychiatry 51(6):485–492 https://doi.org/10.1016/S0006-3223(01)01335-X

Freund, T. F., Katona, I. (2007). Perisomatic inhibition. Neuron.56(1):33–42 https://doi.org/10.1016/j.neuron.2007.09.012

Frischknecht, R., Gundelfinger E, D. (2012). The brain's extracellular matrix and its role in synaptic plasticity. Adv Exp Med Biol 970:153-171. https://doi.org/10.1007/978-3-7091-0932-8_7

Garcia, E., Mills, A., 2002. Getting around lethality with inducible Cre-mediated excision. Seminars in Cell & Developmental Biology 13, 151158. http://dx.doi.org/10.1016/S1084-9521(02)00019-8

Geyer, M. A., Braff, D. L. (1987). Startle habituation and sensorimotor gating in schizophrenia and related animal models. Schizophrenia Bulletin, 13(4), 643-668. http://dx.doi.org/10.1093/schbul/13.4.643

Giamanco, K. A., & Matthews, R. T. (2012). Deconstructing the perineuronal net: cellular contributions and molecular composition of the neuronal extracellular matrix. Neuroscience, 218, 367–84. https://doi.org/10.1016/j.neuroscience.2012.05.055

Glowa, J. R., Carl, T.H., 1994**.** Differences in response to an acoustic startle stimulus among forty-six rat strains. Behavior Genetics, Vol 24, issue 1, 79-84**.** https://doi.org/10.1007/BF01067931

Gogolla, N., Caroni, P., Lüthi, A., & Herry, C. (2009). Perineuronal nets protect fear memories from erasure. Science (New York, N.Y.), 325(5945), 1258–61. https://doi.org/10.1126/science.1174146

Golgi, C., 1898. Intorno alla struttura delle cellule nervose. Boll Soc Med-chir Pavia 1:1-14 https://doi.org/10.1016/S0167-8760(03)00019-9

Graham F. (1975) The more or less startling effects of weak prestimuli. Psychophysiology 12:238-248. http://doi.org/10.1111/j.1469-8986.1975.tb01284.x

Hanada, S., Mita, T., Nishino, N. & Tanaka, C. (1987). [3H]muscimol binding sites increased in autopsied brains of chronic schizophrenics. *Life Sci.* 40(3):259–266 (1987). https://doi.org/10.1016/0024-3205(87)90341-9

Haig, A.R., Gordon, E., De Pascalis V., Meares, R.A., Bahramali, H., Harris, A. (2000). Gamma activity in schizophrenia: evidence of impaired network binding? Clin Neurophysiol. 111(8):1461–1468 https://doi.org/10.1016/S1388-2457(00)00347-3

Heckers, S., Stone, D., Walsh, J., Shick, J., Koul, P., Benes, F. M. (2002). Differential hippocampal expression of glutamic acid decarboxylase 65 and 67 messenger RNA in bipolar disorder and schizophrenia. Archives of General Psychiatry. 59(6):521–529 https://doi.org/10.1001/archpsyc.59.6.521

Hendry, S. H., Jones, E. G., Hockfield, S., & McKay, R. D. (1988). Neuronal populations stained with the monoclonal antibody Cat-301 in the mammalian cerebral cortex and and thalamus. The Journal of Neuroscience, 8(2), 518-42. https://doi.org/10.1523/JNEUROSCI.08-02-00518.1988

Heinrichs, R. W., & Zakzanis, K. K. (1998). Neurocognitive deficit in schizophrenia: A quantitative review of the evidence. *Neuropsychology, 12*(3), 426-445. https://doi.org/10.1037/0894-4105.12.3.426

Hensch, T. K., 2005. Critical period plasticity in local cortical circuits. Nat Rev Neurosci, Nov;6(11):877-88. https://doi.org/10.1038/nrn1787

Hoffman, H. S., Ison, J. R., 1980. Reflex modification in the domain of startle: I. Some empirical findings and their implications for how the nervous system processes sensory input. Psychol. Rev., 87, 175-189. http://dx.doi.org/10.1037/0033-295X.87.2.175

Holm, S. (1979) A simple sequentially rejective multiple test procedure. Scand J Statistics 6:65-70

Howland, J. G., Greba, Q., Paylor, J. W., Zabder, N. K., Murray, I. R., Winship, I. R. (2016). Degradation of perineuronal nets in medial prefrontal cortex impairs prepulse inhibition and crossmodal object recognition memory: implications for schizophrenia. Program No. 845.23. Neuroscience Meeting Planner. San Diego, CA: Society for Neuroscience.

Hoy, R., Nolen, T., Brodfuehrer, P. (1989). The neuroethology of acoustic startle and escape in flying insects. J Exp Biol 146:287-306

Ison, J. R., Pinckney, L. A., 1983. Reflex inhibition in humans: sensitivity to brief silent periods in white noise. Perception & Psychophysics, Vol 34, issue 1, 84-88.

Hylin, M. J., Orsi, S. A., Moore, A. N., & Dash, P. K. (2013). Disruption of the perineuronal net in the hippocampus or medial prefrontal cortex impairs fear conditioning. Learning & Memory (Cold Spring Harbor, N.Y.), 20(5), 267–73. https://doi.org/10.1101/lm.030197.112

Kumari V., Soni, W., Matthew, W. M., Sharma, T. (2000). Prepulse inhibition of the startle response in men with schizophrenia: effects of age on onset of illness, symptoms, and medication. *Arch Gen Psychuatri 57*(6)609-14. http://psycnet.apa.org/doi/10.1001/archpsyc.57.6.609

Kwok, J. C. F., Dick, G., Wang, D., & Fawcett, J. W. (2011). Extracellular matrix and perineuronal nets in CNS repair. Developmental Neurobiology, 71(11), 1073-89. https://doi.org/10.1002/dneu.20974

Landis, C., Hunt, W. A., 1939. *The Startle Pattern*. Farrar and Rinehart, New York. https://doi.org/10.1192/bjp.85.357.808-b

Lanton, R. A. (2015). Optical imaging of intrinsic signals during ocular dominance plasticity in a conditional aggrecan knockout mice. University of Oslo.

Lawrie, S. M., Buechel, C., Whalley, H. C., Frith, C. D., Friston, J., Johnstone, E. C. (2002). Reduced frontotemporal functional connectivity in schizophrenia associated with auditory hallucinations. *Biol Psychyatry* Vol 51, Issue 12, 1008-1011. https://doi.org/10.1016/S0006-3223(02)01316-1

Le, Y. Z., Zheng, W., Rao, P. C., Zheng, L., Anderson, R. E., Esumi, N., Zack, D. J., Zhu, M. (2008). Invest Ophthalmol Vis Sci 49(3):1248-53

Lensjø, K. K., Christensen, A. C., Tennøe, S., Fyhn, M., & Hafting, T. (2017). Differential Expression and Cell-Type Specificity of Perineuronal Nets in Hippocampus, Medial Entorhinal Cortex, and Visual Cortex Examined in the Rat and Mouse. Eneuro, 4(3), ENEURO.0379-16.2017. https://doi.org/10.1523/ENEURO.0379-16.2017

Lensjø, K. K., Lepperød, M. E., Dick, G., Hafting, T., & Fyhn, M. (2017). Removal of Perineuronal Nets Unlocks Juvenile Plasticity Through Network Mechanisms of Decreased Inhibition and Increased Gamma Activity. The Journal of Neuroscience, 37(5), 1269–1283. https://doi.org/10.1523/JNEUROSCI.2504-16.2016

Lewis, D. A, Glantz, L. A., Pierri, J. N., Sweet R. A. (2003). Altered cortical glutamate neurotransmission in schizophrenia: evidence from morphological studies of pyramidal neurons. *Ann N Y Acad Sci. 1003*:102–112 https://www.ncbi.nlm.nih.gov/pubmed/14684438

Litchenstein, P., Yip, B. H., Björk, C., Pawitan, Y., Cannon, T. D., Sullivan, P. F., Hultman, C. M. (2009). Common genetic determinants of schizophrenia and bipolar disorder in Swedish families: a population-based study. *Lancet 373*(9659):234-9 https://doi.org/10.1016/S0140-6736(09)60072-6

Liu, H., Gao, P, F., Xu, H, W., Yu, T., Yao, J, P., Yin, Z, Q. (2013). Perineuronal nets increase inhibitory GABAergic currents during the critical period in rats. Int J Ophantamol 6:120-125. https://doi.org/10.3980/j.issn.2222-3959.2013.02.02

Lodge, D. J., Behrens, M. M., & Grace, A. A. (2009). A loss of parvalbumin-containing interneurons is associated with diminished oscillatory activity in an animal model of schizophrenia. The Journal of Neuroscience : The Official Journal of the Society for Neuroscience, 29(8), 2344–54. https://doi.org/10.1523/JNEUROSCI.5419-08.2009

Matuszko, G., Curreli, S., Kaushik, R., Becker, A., Dityatev, A. (2017). Extracellular matrix alteration in the ketamine model of schizophrenia. Neuroscience 350:13-22 https://doi.org/10.1016/j.neuroscience.2017.03.010

Marwaha, S, Johnson, S. (2004). Schizophrenia and employment – a review. *Soc Psychiatry Psychiatr Epidemiol 39*(5):337-49 https://doi.org/10.1007/s00127-004-0762-4

Meyer-Lindberg A. S., Olsen, R. K., Kohn, P. D. (2005). Regionally specific disturbance of dorsolateral prefrontal-hippocampal functional connectivity in schizophrenia. Arch Gen Psychiatry 62(4):379-386 https://jamanetwork.com/journals/jamapsychiatry/fullarticle/208512

MacDonald III, A. W., Carter, C. S., Kerns, J. G., Ursu, S., Barch, D. M., Holmes, A. J., ... & Cohen, J. D. (2005). Specificity of prefrontal dysfunction and context processing deficits to schizophrenia in never-medicated patients with first-episode psychosis. *American Journal of Psychiatry*, *162*(3), 475-484. https://doi.org/10.1176/appi.ajp.162.3.475

MacDonald, A. W., Schulz, S. C. (2009). What we know: findings that every theory of schizophrenia should explain. *Schizophr. Bull. 35*, 493–508. https://doi.org/10.1093/schbul/sbp017

Mauney, S. A., Athanas, K. M., Pantazopoulos, H., Shaskan, N., Passeri, E., Berretta, S., & Woo, T. U. W. (2013). Developmental pattern of perineuronal nets in the human prefrontal cortex and their deficit in schizophrenia. *Biological psychiatry*, *74*(6), 427-435. https://doi.org/10.1016/j.biopsych.2013.05.007

Meighan, S. E., Meighan, P. C., Choudhury, P., Davis, C. J., Olson, M. L., Zornes, P. A., … Harding, J. W. (2006). Effects of extracellular matrix-degrading proteases matrix metalloproteinases 3 and 9 on

spatial learning and synaptic plasticity. Journal of Neurochemistry, 96(5), 1227–41. https://doi.org/10.1111/j.1471-4159.2005.03565.x

Murray, A. J., Woloszynowska-Fraser, M. U., Ansel-Bollepalli, L., Cole, K. L. H., Fogetti, A., Crouch, B., riedel, G., Wulff, P. (2015). Parvalbumin-positive interneurons of the prefrontal cortex support working memory and cognitive flexibility. Sci Rep 5:16778 http://doi.org/10.1038/srep16778

Nowicka, D., Soulsby, S., Skangiel-Kramska, J., Glazewski, S. (2009). Parvalbumin-containing neurons, perineuronal nets and experience-dependent plasticity in murine barrel cortex. *Eur. J. Neurosci.* 30, 2053–2063 https://doi.org/10.1111/j.1460-9568.2009.06996.x

Nusbaum, M. P., Contreras, D. (2004). Sensorimotor gating: startle submits to presynaptic inhibition. Current Biology, 14(6):247-249 https://www.sciencedirect.com/science/article/pii/S0960982204001514

Morrison, D. J., Rashid, A. J., Yiu, A. P., Yan, C., Frankland, P. W., Josselyn, S. A. (2016). Parvalbumin interneurons constrain the size of the lateral amygdala engram. Neurobiol Learn Mem 135:91-99 https://doi.org/10.1016/j.nlm.2016.07.007

Murray, A. J., Woloszynowska-Fraser, M. U., Ansel-Bollepalli, L., Cole, K. L. H., Foggetti, A., Crouch, B., … Wulff, P. (2015). Parvalbumin-positive interneurons of the prefrontal cortex support working memory and cognitive flexibility. Scientific Reports, 5(1), 16778. https://doi.org/10.1038/srep16778

Paxinos, G., Franklin, K. B. J. (2001). The mouse brain in stereotaxic coordinates, second edition. Academic press

Paylor, R., Crawley, J.N. Inbred strain differences in prepulse inhibition of the mouse startle response. Psychopharmacology (Berl) 132(2):169-80

Perry, T. L., Kish, S. J., Buchanan, J., Hansen, S. (1979). Gamma-aminobutyric-acid deficiency in brain of schizophrenic patients. Lancet (London, England). 1(8110):237–239

Pilz, P. K., Schnitzler, H.-U., Menne, D., 1987. Acoustic startle threshold of the albino rat (Rattus norvegicus). *Journal of Comparative Psychology*, *101*(1), 67-72. http://psycnet.apa.org/doi/10.1037/0735-7036.101.1.67

Pizzorusso, T., Medini, P., Berardi, N., Chierzi, S., Fawcett, J. W., & Maffei, L. (2002). Reactivation of ocular dominance plasticity in the adult visual cortex. Science (New York, N.Y.), 298(5596), 1248–51. https://doi.org/10.1126/science.1072699

Pizzorusso, T., Medini, P., Landi, S., Baldini, S., Berardi, N., Maffei, L. (2006). Structural and functional recovery from early monocular deprivation in adult rats. Proc Natl Acad Sci U S A. May 30;103(22):8517-22. https://doi.org/10.1073/pnas.0602657103

Plappert, C. F., Pilz, P. K. D., & Schnitzler, H.-U. 1993. Acoustic startle response and habituation in freezing and nonfreezing rats. *Behavioral Neuroscience, 107*(6), 981-987. http://psycnet.apa.org/doi/10.1037/0735-7044.107.6.981

Ralph-Williams, R. J., Lehmann-Masten, V., Geyer, M. A. (2003). *Dopamine D1 rather than D2 receptor agonists disrupt prepulse inhibition of startle in mice. Neuropsychopharmacology 28*(1):108-18 https://doi.org/10.1038/sj.npp.1300017

Ralph, R. J., Caine S. B. (2005). *Dopamine D1 and D2 agonist effects on prepulse inhibition and locomotion: comparison of Sprague-dawley rats to swiss-webster, 129X1/SvJ, C57BL/6, and DBA/2J mice. J Pharmacol Exp Ther 312*(2):733-41 https://doi.org/10.1124/jpet.104.074468

Ronca, S. E., Smith, J., Koma, T., Miller, M. M., Yun, N., Dineley, K. T., Paessler, S. (2017). *Mouse model of Neurological complications resulting from encephalitic alphavirus infection. Front Microbiol 8*:188 https://doi.org/10.3389/fmicb.2017.00188

Scudder, S. L., Baimel, C., Macdonald, E. E., Carter, A. G. (2018). Hippocampal-evoked feed-forward inhibition in the nucleus accumbens. J Neurosci pii: 1971-18 https://doi.org/10.1523/JNEUROSCI.1971-18.2018

Slaker, M., Churchill, L., Todd, R. P., Blacktop, J. M., Zuloaga, D. G., Raber, J., … Sorg, B. A. (2015). Removal of perineuronal nets in the medial prefrontal cortex impairs the acquisition and reconsolidation of a cocaine-induced conditioned place preference memory. The Journal of Neuroscience: The Official Journal of the Society for Neuroscience, 35(10), 4190–202. https://doi.org/10.1523/JNEUROSCI.3592-14.2015

Swerdlow, N. R., Geyer. M. A. (1998). Using an animal model of deficient sensorimotor gating to study the pathophysiology and new treatments of Schizophrenia. https://doi.org/10.1093/oxfordjournals.schbul.a033326

Swerdlow, N. R., Weber, M., Qu, Y., Light A. G., Braff, D. L. (2008). *Realistic expectations of prepulse inhibition in translational models for schizophrenia research. Psychopharmacology, Vol 199,* Issue 3, 331-388. https://doi.org/10.1007/s00213-008-1072-4

Swerdlow, N. R., Braff, D. L., Geyer, M, A. (2016). Sensorimotor gating of the startle reflex: what we said 25 years ago, what has happened since then, and what comes next. *J Psychopharmacol*. (11):1072-1081 https://doi.org/10.1177%2F0269881116661075

Swerdlow, N. R., Bhakta, S. G., Rana, B. K., Kei, J., Chou, H. H., Talledo, J. A. (2017). Sensorimotor gating in healthy adults tested over a 15 year period. *Biol Psychol 123*:177-186. https://doi.org/10.1016/j.biopsycho.2016.12.011

Takahashi, K., Nagai, T., Kamei, H., Maeda, K., Matsuya, T., Arai, S., Mizoguchi, H., Yoneda, T., Nabeshima., Takuma, K., Yamada, K. (2007). *Neural circuits containing pallidotegmental GABAergic neurons are involved in the prepulse inhibition of the startle reflex in mice. Biol Psychiatry 62*(12):148-57 https://doi.org/10.1016/j.biopsych.2006.06.035

Tamas, G., Buhl, E. H., Lorincz, A., Somogyi, P. (2000). Proximally targeted GABAergic synapses and gap junctions synchronize cortical interneurons. Nat Neurosci. 3(4):366–371 https://doi.org/10.1038/73936

Thompson, E. H., Lensjø, K. K., Wigestrand, M. B., Malthe-Sørenssen, A., Hafting, T., & Fyhn, M. (2018). Removal of perineuronal nets disrupts recall of a remote fear memory. Proceedings of the National Academy of Sciences of the United States of America, 115(3), 607–612. https://doi.org/10.1073/pnas.1713530115

The Schizophrenia Commission – Rethink Mental Illness, the mental health charity. (2012). Retrieved August 20, 2018, from https://www.rethink.org/about-us/the-schizophrenia-commission

Tiihonen, J., Lönnqvist, J., Wahlbeck, K., Klaukka, T., Niskanen, L., Tanskanen, A., Haukka, J. (2009). 11-year follow-up of mortality in patients with schizophrenia: a population-based cohort study (FIN11 study). *Lancet 374*(9690):620-7 https://doi.org/10.1016/S0140-6736(09)60742-X

Uhlhaas, P.J., Haenschel, C., Nikolic, D., Singer W. (2008). The Role of Oscillations and Synchrony in Cortical Networks and Their Putative Relevance for the Pathophysiology of Schizophrenia. Schizophr Bull. 34(5):927-43 https://doi.org/10.1093/schbul/sbn062

Valsamis, B., Schmid, S. (2011). *Habituation and prepulse inhibition of acoustic startle in rodents. Neuroscience 55* https://doi.org/10.3791/3446

Wang, D., Fawcett, J. (2012). The perineuronal net and the control of CNS plasticity. Cell Tissue Res., 349: 147-160. https://doi.org/10.1007/s00441-012-1375-y

Watanabe, E., Fujita, S. C., Murakami, F., Hayashi, M., & Matsumura, M. (1989). A monoclonal antibody identifies a novel epitope surrounding a subpopulation of the mammalian central neurons. Neuroscience, 29(3), 645-57. https://doi.org/10.1016/0306-4522(89)90137-1

Wecker, J. R., Ison, J. R., 1986. Effects of motor activity on the elicitation and modification of the startle reflex in rats. Animal Learning & Behavior. Issue 3, 287-292 https://doi.org/10.3758/BF03200069

Weinberger, D. R., Berman, K. F. (1996). Prefrontal function in schizophrenia: confounds and controversies. *Philos. Trans. R. Soc. Lond. B Biol. Sci.* 351(1346):1495–1503 https://doi.org/10.1098/rstb.1996.0135

Weike, A. L., Bauer, U., Hamm, A. O. (2000). Effective neuroleptic medication removes prepulse inhibition deficits in schizophrenia patients. Biol Psychiatry Vol 47, Issue 1, 61-70. https://doi.org/10.1016/S0006-3223(99)00229-2

Williams, S., Boksa, P. (2010). Gamma oscillations and schizophrenia. J Psychiatry Neurosci 35(2):75-7. https://dx.doi.org/10.1503%2Fjpn.100021

Willot, J. F., Tanner, L., O'Steen, J., Kphnson, K. R., Bogue, M. A., Gagnon, L. (2003). *Acoustic startle and prepulse inhibition in 40 inbred strains of mice. Behav Neurosci 117*(4):716-27 http://psycnet.apa.org/doi/10.1037/0735-7044.117.4.716

Wolkin, A., Sanfilipo, M., Wolf A. P., Angrist, B., Brodie, J. D., Rotrosen, J. (1992). Negative symptoms and hypofrontality in chronic schizophrenia. *Arch. Gen. Psychiatry* 49(12):959–965 https://doi.org/10.1001/archpsyc.1992.01820120047007

Whittington, M. A., Traub, R.D., Jefferys, J, G. (1995). Synchronized oscillations in interneuron networks driven by metabotropic glutamate receptor activation. Nature. 373(6515):612–615 https://doi.org/10.1038/373612a0

Yeomans, J-S., Frankland, P. W., 1995. The acoustic startle reflex: neurons and connections. Brain Research Reviews, Volume 21, 301-314. https://doi.org/10.1016/0165-0173(96)00004-5

6. Appendix

6.1 List of abbreviations

AAV	Adeno-associated virus
ASR	Acoustic startle reflex
ChABC	ChondroitinaseABC
CNS	Central nervous system
CSPGs	Chondroitin sulfate proteoglycans
ECM	Extracellular matrix
GFP	Green fluorescent protein
HET CRE	Heterozygous ACAN floxed mice expressing Cre
HOMO CRE	Homozygous ACAN floxed mice expressing Cre
IL	Infralimbic
ISI	Interstimulus interval
ITI	Intertrial interval
mPFC	Medial prefrontal cortex
PBS	Phosphate-buffered saline
PFA	Paraformaldehyde
PNN	Perineuronal nets
PPI	Prepulse inhibition
PrL	Prelimbic
PV+	Parvalbumin-expressing
PV+ Cell	Parvalbumin-expressing inhibitory interneurons
SCZ	Schizophrenia
SPL	Sound pressure level
WFA	Wisteria floribunda agglutinin

6.2 Solutions used for histology & immunohistochemistry

10X PBS

80g of NaCl

2.0g of KCl

14.4g of Na_2HPO_4

2.4g of KH_2PO_4

Dissolved in 800 mL dH_20, adjust pH to 7.4 and volume to 1L.

Dilute 1:10 with dH_2O for 1X PBS solution

Tris-HCL 0.05M

6.6g

1L H_2O, adjust pH to 7.6

4% Paraformaldehyde (PFA)

40 g PFA

1L 1X PBS

Warm up to 50-60 °C and leave for 3-4 hours stirring for dissolving and filter before use.

6.3 WFA & GFP Immunostaining with DAPI

Wash sections 3x5 min in PBS ~ 200 rpm

Block sections in 1% BSA and 0.3% Triton X-100 in 1X PBS for 60 min in room temperature.

Incubate sections with WFA-biotin (1:200) and primary chicken GFP antibody (1:2000) in block solution (1%BSA and 0.3% Triton-X in 1xPBS) over night.

Wash 3x5 min i PBS

Incubate sections with secondary antibodies Alexa 488 anti-chicken (1:400) and streptavidin alexa-594 (1:1000) in 1xPBS, for two hours on the shaker. Remember to shield from light.

Wash 3x5 min in 1xPBS

Mount sections on superfrost slides (or 1% gelatin covered glass)

Allow slides to dry for 20-30 minutes in the dark.

Rinse in ddH2O and let slides dry slightly.

Add DAPI mounting solution